UNIVERSITY OF TARTU

FACULTY OF SCIENCE AND TECHNOLOGY

INSTITUTE OF TECHNOLOGY

The function of ABA transporters during low humidity-induced stomatal closure in

*Arabidopsis thaliana***.**

Bachelor's Thesis

12 ECTS

Turgay Hasanov

Supervisors:

Dr. Rainer Waadt,

Prof. Dr. Hannes Kollist

Tartu 2021

ABSTRACT

The function of ABA transporters during low humidity-induced stomatal closure in *Arabidopsis thaliana*.

Plants are important for our nature and for all living things. These organisms can produce food, energy and several natural products from carbon dioxide and solar energy. Plants take up CO_2 from the air in exchange for water via small pores called stomata on the leaf surface. These stomata are formed by pairs of cells, called guard cells. As plants are sessile organisms, they cannot move and need to adapt their physiology to the imposed environmental conditions. Drought is one of the major problems caused by climate change and guard cell physiology plays an important role in regulating stomatal apertures and the plant water content. For stomatal aperture regulation under limiting water conditions, the plant hormone abscisic acid (ABA) plays a major role. To understand guard cell physiology and the role of ABA in the plant response to low air humidity, defined as the Vapor Pressure Deficit (VPD) between plants and the atmosphere, we performed gas exchange analyses using *Arabidopsis thaliana* wild type plants and mutants in which ABA transporter genes were disrupted. Among the tested mutants, we observed a slower VPD response in a mutant in which the *ABCG22* gene was disrupted. However, we did not observe clearly altered high VPD responses of *abcg25*, *abcg31*, *abcg40*, *npf4.6* and *npf5.2* ABA transporter mutants. This may be due to a high functional overlap between several ABA transporter genes. We also performed gene expression analyses of ABA transporter genes using the Genevestigator tool. This allowed us to propose the testing of additional ABA transporter genes that might be relevant for the high VPD response in Arabidopsis.

Keywords: ABA, ABA transport, guard cells, stomatal closure, stomatal conductance, VPD response.

CERCS: B310 Physiology of vascular plants

Kokkuvõte

ABA transporterite roll *Arabidopsis thaliana* õhulõhede sulgumises madala õhuniiskuse toimel

Taimed on olulised looduse ja kõigi elusorganismide jaoks. Nad toodavad toitu, energiat ja muid looduslikke produkte süsinikdioksiidist ning päikseenergiast. Taimede CO_2 omastamine õhust toimub samaaegselt vee aurustumisega läbi õhulõhede, väikeste pooride lehepinnal. Õhulõhed moodustuvad kahest sulgrakust. Kuna taimed on paiksed organismid ja ei liigu, peavad nad füsioloogiliselt kohastuma ümbritseva keskkonnaga. Üks olulisemaid kliimamuutustega kaasnevaid probleeme on põud; sulgrakkude füsioloogia on väga oluline õhulõhede avatuse ning taimede veesisalduse reguleerimisel. Taimehormoon abstsiishape (ABA) mängib olulist rolli õhulõhede avatuse regulatsioonis veestressi tingimustes. Mõistmaks sulgrakkude füsioloogiat ja ABA rolli taimede vastuses madalale õhuniiskusele, st õhu niiskusvajakule (VPD, vapor pressure deficit), viisime läbi gaasivahetuskatsed, kasutades *Arabidopsis thaliana* metsiktüüpi taimi ja mutante, milles ABA transporterite geenid olid rikutud. Me ei leidnud olulisi muutusi kõrge VPD-toimelises vastuses järgmistes ABA transporterite mutantides: *abcg25, abcg31, abcg40, npf4.6, npf5.2*. Selle tulemuse põhjuseks võib olla suur funktsionaalne kattuvus ABA transporterite seas. Kasutades Geneinvestigator'it, analüüsisime ka ABA transporterite geeniekspressioone. Nende analüüside tulemusel pakume testimiseks uusi ABA transportereid, mis võivad osutuda oluliseks Arabidopsise VPD-vastuses.

Table of contents

Abbreviations

ABA - ABSCISIC ACID

ABA2 - ARABIDOPSIS THALIANA ABA DEFICIENT 2

ABA-GE - ABA glucose ester

ABC - ATP-BINDING CASETTE

AAO3 - ABSCISIC ALDEHYDE OXIDASE 3

AKT1 - ARABIDOPSIS K^+ TRANSPORTER 1

AKT2/3 - ARABIDOPSIS K^+ TRANSPORTER 2/3

AMY3 - ALPHA-AMYLASE 3

BAM1 - BARELY ANY MERISTEM1

BAM3 - BARELY ANY MERISTEM3

BG1 - BETA GLUCOSIDASE 18

BG2 - BETA GLUCOSIDASE 33

BLUS1 - BLUE LIGHT SIGNALING1

CRY - CRYPTOCHROME

COP1 - CONSTITUTIVE PHOTOMORPHOGENIC 1

DTX50 - DETOXIFICATION EFFLUX CARRIER 50

GORK - GATED OUTWARDLY RECTIFYING K^+ CHANNEL

GHR1 - GUARD CELL HYDROGEN PEROXIDE-RESISTANT1

H^+-ATPase - ATP dependent H^+-transporter

K^+_{in} - K^+ inward channel

KAT1 - POTASSIUM CHANNEL IN *ARABIDOPSIS THALIANA* 1

KAT2 - POTASSIUM CHANNEL IN *ARABIDOPSIS THALIANA* 2

NCED - NINE-CIS - EPOXYCAROTENOID DIOXYGENASE

NCED3 - NINE-CIS - EPOXYCAROTENOID DIOXYGENASE3

NPF - NITRATE TRANSPORTER 1/ PEPTIDE TRANSPORTER FAMILY

OST1 - OPEN STOMATA 1

PAR - PHASEIC ACID REDUCTASE

PHOT1 and PHOT2 - Phototropins

PCR - Polymerase Chain Reaction

PP1 - PROTEIN PHOSPHATE TYPE 1

PP2C - PROTEIN PHOSPHATE TYPE 2C

PYR1 - PYRABACTIN RESISTANCE 1

PYL - PYRABACTIN RESISTANCE-LIKE

QUAC1 - QUICK ACTIVATING ANION CHANNEL 1

RBOH - RESPIRATORY BURST OXIDASE HOMOLOG

RCAR - REGULATORY COMPONENT OF ABA RECEPTOR

RH – Relative Humidity

ROS - Reactive Oxygen Species

SLAC1 - SLOW ANION CHANNEL ASSOCIATED 1

SLAH3 - SLAC1 HOMOLOGUE 3

SDR - SHORT CHAIN DEHYDROGENASE/REDUCTASE-LIKE

TAE - Tris/Acetate/EDTA

VPD - Vapor Pressure Deficit

Introduction

Plants are multicellular organisms with an extraordinary ability to produce food and energy from carbon dioxide and solar energy. Plants take up CO_2 from the air through stomata, small pores on the leaf and stem surface. These stomatal pores regulate the gas exchange between the environment and the plant. A stomatal pore is surrounded by a pair of guard cells in the epidermis, which control the opening and closing of stomata (Schroeder et al., 2001). Since plants are not able to move, they must adjust their physiology according to environmental conditions. The regulation of stomatal apertures helps plants to sense and cope with their environment, such as weather, nutrients, and pathogens, to maximize their fitness. Plants need to respond to environmental stresses, and one of them is drought. In respond to drought, plants use stomata to regulate water contentment. Due to climate change (increase in temperature, heat waves, and water shortage), drought is and will be a major problem. There are two types of drought: 1) drought in the soil and 2) low air humidity, which is also defined as Vapor Pressure Deficit (VPD) (Sussmilch and McAdam, 2017a). The plant's water loss means that it cannot take up nutrients, because it needs water flow. When there is drought, stomata close, preventing CO_2 uptake, which is required for photosynthesis, and this affects the growth of the plant. Drought is bad in two ways: It inhibits nutrient uptake from the soil, but it also inhibits CO_2 uptake from the leaves. Guard cell physiology and stomatal aperture regulation are essential to regulate the plant water status. Like in all organisms, communication is necessary, and this is mediated by signaling between the plant organs. For example, in dry-soil conditions, root-derived signals help shoot growth to adapt to the environment (Takahashi et al., 2018a).

To study the guard cell physiology and VPD response, I performed gas exchange analyses. Gas exchange is a process in which water vapor and oxygen leaves, and carbon dioxide enter the plant leaves (Kollist et al., 2007). A gas exchange system allows to measure the gas exchange between the plant and the atmosphere. Plant hormones (phytohormones) play essential roles in plant development, plant adaptation to environmental stresses, and stomatal aperture regulation. One of the most important phytohormones for stomatal regulation is abscisic acid (ABA) (Chen et al., 2020b). In this study, I focused on analyzing ABA transporter mutants during low humidity (high VPD)-induced stomatal closure in *Arabidopsis thaliana* using gas exchange analyses. The current study was performed in the Plant Signal Research Group at the Institute of Technology.

1. Literature review

1.1. The role of ABA during drought stress

It has been shown that ABA is vital for mediating drought stress responses by closing stomata (Ali et al., 2020). Since ABA biosynthesis enzymes and transporters are expressed in vascular tissues, it is thought that vascular tissue synthesized ABA is key to the drought response (Sussmilch and McAdam, 2017b). Also, ABA-dependent and ABA-independent regulatory systems can regulate the drought stress responses (Nakashima et al., 2014; Takahashi et al., 2018a). It is still not clear, how ABA is moving from vascular tissues to guard cells, roots, and other tissues. In drought, the condition of the soil and atmosphere varies. A plant can sense the amount of water shortage in the soil under the stress condition and carry signals from roots to leaves to induce ABA accumulation (Christmann et al., 2007). The vascular system in the plant helps to connect the root with the shoot. CLAVATA3/EMBRYO-SURROUNDING REGION-RELATED 25 (CLE25) is a signaling peptide that regulates the synthesis of ABA in response to drought. The CLE25 peptide is expressed in roots and moves to leaves where it activates the receptor-like kinases BARELY ANY MERISTEM 1 (BAM1) and BARELY ANY MERISTEM 3 (BAM3) (Takahashi et al., 2018c). BAM1 and BAM3, in turn, trigger a yet uncharacterized signaling cascade to induce the expression of NCED3 in the leaf vasculature, promoting the biosynthesis of ABA. Recent studies have reported reactive oxygen species (ROS), Ca^{2+}, mRNAs, hydraulic signals, and phytohormone movements (Choi et al., 2017; Kudla et al., 2018) help to regulate drought stress responses as well. Turgor loss in roots activates ABA biosynthesis in leaves via CLE25, hydraulic signals, and Ca^{2+} that induce the expression of NINE CIS EPOXYCAROTENOID DIOXYGENASE3 (NCED3) (Chen et al., 2020a; Christmann et al., 2007; Endo et al., 2008; Takahashi et al., 2018b) in the vasculature of the dehydrated leaves. Also, sulfate can mediate stomatal closure via ABA accumulation and Reactive Oxygen Species (ROS) (Batool et al., 2018). In general, we can observe that plants can regulate the stomatal aperture at different places via several signals in stress conditions.

1.2. Importance of stomata in plant functioning

Stomata formed by two guard cells are small pores on the surface of the leaves that allow CO_2 uptake and water loss through transpiration. Because plants cannot move, they need to adapt to their environmental conditions. The development of a gas impermeable cuticle helps plant tissues to avoid losing water in unfavorable conditions. To enable photosynthesis, which mainly occurs in mesophyll cells, CO_2 needs to enter the plant leaves via stomata. Environmental signals also affect stomatal development. Plants evolved mechanisms to adapt quickly to the environment, such as stomatal density changes in young plant leaves and quick modification of stomatal apertures (Chater et al., 2014).

Guard cells are connected to the environment. They can sense internal and external stimuli to regulate stomatal apertures. Stomatal opening and closing are guided by an increase and decrease of the guard cell turgor pressure. Stomatal opening is caused by environmental factors, such as high air humidity, light, and low atmospheric CO_2 concentration. During the stomatal opening, guard cells swell by taking up osmotically active compounds and water. Opposite factors trigger stomatal closure as it was in stomatal opening, for example, low air humidity, high atmospheric CO_2, and darkness. Stomatal closing is induced by water release from guard cells and the reduction of their turgor pressure. ABA, a phytohormone that regulates plant growth and development in response to water limiting conditions, functions as a major regulator of stomatal closure. Guard cell responses are regulated by several interconnected signal transduction networks, including ABA, CO_2, and Ca^{2+} (Kim et al., 2010). The underlying signal transduction processes are regulated by protein kinases and phosphatases that control the activity of ion channels and transporters for modulating guard cell turgor and associated stomatal apertures.

1.3. Stomatal opening

Stomatal opening ensures CO_2 flow to mesophyll cells for photosynthetic CO_2 fixation and transpiration in plants. Opening of stomata is induced by red and blue light. In guard cells, blue light photoreceptors are phototropin (PHOT1and PHOT2) and cryptochrome (CRY1 and CRY2). It has been shown that stomatal development intercedes through the CRYPTOCHROME-PYHTOCHROME and CONSTITUTIVE PHOTOMORPHOGENIC 1 (COP1) signaling system

and the mitogen-activated protein kinase signaling pathway (Araújo et al., 2011). Blue light induces the activation and autophosphorylation of the blue-light receptor serine/threonine (Ser/Thr) protein kinases PHOT1 and PHOT2 to promote the stomatal opening. Then phototropins phosphorylate the protein kinase BLUE LIGHT SIGNALING1 (BLUS1), which transfers the blue-light signal further to PROTEIN PHOSPHATASE TYPE 1 (PP1). The blue light signal response leads finally to the Plasma Membrane (PM) H^+-ATPase (AHAs) activation via phosphorylation of its penultimate Thr residue and interaction with 14-3-3 proteins. However, the protein kinase that directly phosphorylates and activates the H^+-ATPase at the penultimate Thr residue is currently unknown (Inoue and Kinoshita, 2017). Upon activation, the H^+-ATPase pumps protons (H^+) out of the guard cells. The H^+-ATPase AHA1 (Autoinhibited H^+-ATPase) (Falhof et al., 2016) is essential in the blue-light stomatal opening, and AHA1 activity induces hyperpolarization of the guard cell plasma membrane. This, in turn, activates voltage-gated K^+-channels leading to K^+ uptake into guard cells (Yamauchi et al., 2016) (**Figure 1**, left).

Red light-mediated stomatal opening is linked with reduced intercellular CO_2 concentration and signals generated by mesophyll cells (Roelfsema et al., 2002). Starch has an essential role in stomatal opening. Starch degradation in guard cells provides the energy during the initial 30 minutes of light-induced stomatal opening (Horrer et al., 2016). BAM1 (Beta-AMYLASE 1) and AMY3 (Alpha-AMYLASE 3) are key enzymes that contribute to the degradation of starch in guard cells.
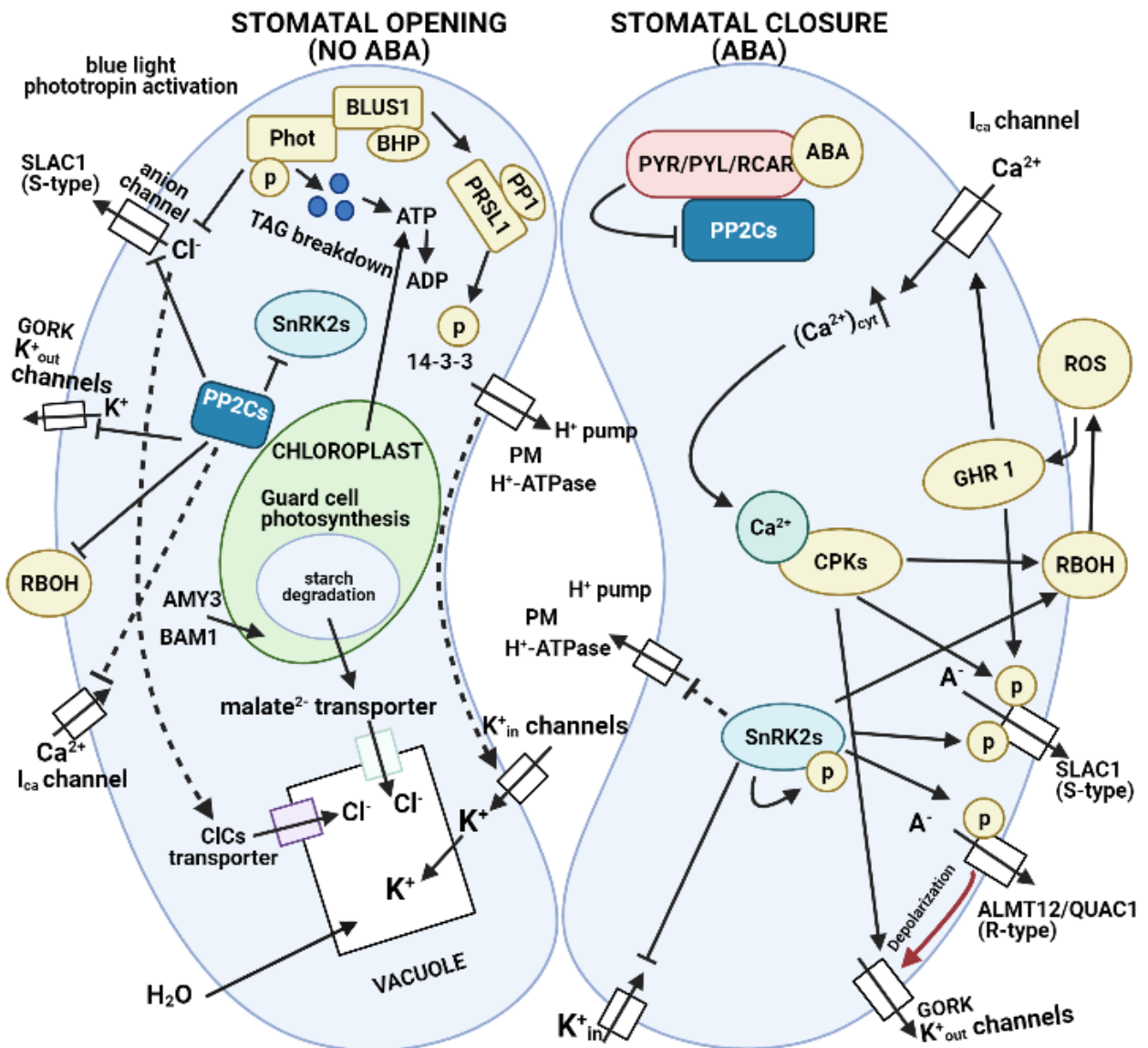
Figure 1. Opening and closing of stomata. (Left) During the stomatal opening, blue light activates phototropins (PHOT) which via a phosphorylation/dephosphorylation cascade mediated by the protein kinase BLUS1 and the phosphatase PP1 leads to the phosphorylation, 14-3-3 binding and activation of the plasma membrane H^+-ATPase. H^+-ATPase-mediated export of H^+ across the guard cells plasma membrane leads to a hyperpolarization of the plasma membrane allows K^+_{in} channels to get activated so that K^+ enters the guard cells. PP2Cs directly inhibit SnRK2s, the SLAC1 anion channel, the GORK K^+_{out} channel, RBOH and indirectly inhibit I_{Ca} channels to inhibit stomatal closure mechanisms. The breakdown of starch promotes the accumulation of malate^{2-} and the synthesis of sugars. BAM1 and AMY3 enzymes contribute to the degradation of starch in guard cells. Other ions, such as NO_3^- and Cl^- also get transported into guard cells and stored in the vacuole. The accumulation of these compounds in guard cells leads to a turgor pressure increase that promotes water influx and stomatal opening. **(Right)** During stomatal

closure and in response to ABA, ABA receptors (PYR/PYL/RCAR) inhibit PP2Cs, leading to the activation of SnRK2s. SnRK2s activate S-type SLAC1 and R-type ALMT12/QUAC1 anion channels and RBOH, inhibit the K^+_{in} channel KAT1 and indirectly the H^+-ATPase. RBOH activation by SnRK2s induces ROS production, which via GHR1 leads to the activation of Ca^{2+}-permeable channels (I_{Ca}) and the anion channel SLAC1. Cytosolic Ca^{2+} activates Ca^{2+}-dependent protein kinases (CPKs) which contribute to the activation of SLAC1, RBOH and the outward-rectifying K^+ channel GORK leading to ion and water efflux from guard cells and stomatal closure. $Malate^{2-}$ is also converted back to starch by gluconeogenic conversion.

In Arabidopsis, K^+ plays a significant role in stomatal aperture regulation. Changes in guard cell turgor depend on ion channel activities across guard cell membranes. When scientists cloned plant ion channels, one plant K^+ channel KAT1 (POTASSIUM CHANNEL IN ARABIDOPSIS THALIANA 1) showed a role in mediating K^+ influx into guard cells (Pilot et al., 2001). KAT1 together with KAT2 (POTASSIUM CHANNEL IN ARABIDOPSIS THALIANA 2), AKT1 (POTASSIUM TRANSPORTER 1), and AKT2/3 (POTASSIUM TRANSPORTER 2/3) function as K^+ channels (Kollist et al., 2014) during stomatal opening.

1.4. Stomatal closure

The closing of stomata downscales water loss in plants. In the plasma membrane of guard cells, anion channels play an essential role in controlling stomata closure. There are two types of anion channels in the plasma membrane of the guard cell: R-type and S-type. R-type anion channels are activated rapidly within 50 ms by depolarization, deactivated by hyperpolarization, and inactivated during prolonged stimulation. S-type anion channels exhibit a slow voltage-dependent activation and deactivation. SLAC1 (SLOW ANION CHANNEL ASSOCIATED 1) was identified as an S-type anion channel, and it is being activated by ABA and cytosolic Ca^{2+}, dependent phosphorylation. The *slac1* mutant shows an impaired response to stomatal closure stimuli, such as ABA and CO_2 (Negi et al., 2008; Vahisalu et al., 2008). In addition to SLAC1, there is another S-type anion channel, SLAH3 (SLAC1 HOMOLOGUE 3), which is expressed in guard cell as well (Huang et al., 2019). QUAC1 (QUICK ACTIVATING ANION CHANNEL 1) (also known as AtALMT12) was identified as the R-type anion channel, which is expressed in guard cells and targeted to the plasma membrane and is activated by malate (Meyer et al., 2010; Sasaki et al., 2010). Both SLAC1 and QUAC1 are activated by the ABA-dependent protein kinase OST1

(OPEN STOMATA 1) (Geiger et al., n.d.; Imes et al., 2013). SLAC1 and QUAC1 activity leads to a depolarization of the guard cell plasma membrane, which activates the K^+-channel GORK, allowing K^+ release from the guard cells (Ache et al., 2000; Hosy et al., 2003). GORK has an essential role in eliminating K^+ ions and causing stomatal closure. Also, Ca^{2+} is an important messenger to trigger stomatal closure. As Ca^{2+} concentration is rising, it is more likely to stimulate CALCIUM-DEPENDENT PROTEIN KINASES (CPKs) that trigger stomatal closure by activating anion channels (Kollist et al., 2014). Ca^{2+} is found in the apoplast and the vacuole. The activation of Ca^{2+}- permeable channels increases the cytoplasmic Ca^{2+} concentration, and Ca^{2+}-permeable channels (I_{Ca}) are stimulated by hyperpolarization in the guard cell plasma membrane. An increase in cytosolic Ca^{2+} concentration is induced by stimuli, such as ABA and CO_2. Ca^{2+} then activates protein kinases that regulate SLAC1 and K^+ channels (Kollist et al., 2014; Siegel et al., 2009). The ABA-activated protein kinase OST1 not only induces the activation of SLAC1 and QUAC1 via phosphorylation (Kollist et al., 2014; Siegel et al., 2009) but also inhibits K^+ uptake via KAT1 (Sato et al., 2009; Takahashi et al., 2013). In addition, OST1 phosphorylates and activates reactive oxygen species (ROS), producing NADPH oxidases/respiratory burst oxidase homolog (RBOH) proteins to regulate growth, and stress responses in guard cells (Sirichandra et al., 2009). The pseudokinase GUARD CELL HYDROGEN PEROXIDE-RESISTANT1 (GHR1) is involved in the ROS-mediated regulation of stomatal responses, and it contributes to the regulation of SLAC1 and Ca^{2+}-channels (Sierla et al., 2018). Overall, the concerted activity of OST1, CPKs, and GHR1 protein kinases and SLAC1, QUAC1, and GORK ion channels induce a decrease in the guard cell turgor pressure, leading to stomatal closure (**Figure 1,** right)**.**

1.5. Gas exchange

For measuring the gas exchange of a whole plant, a proper gas exchange analysis system is required. This should allow us to measure the transpiration and photosynthesis relations and see which external stimuli affect stomatal movements. Stomatal conductance is the flux of CO_2 or water evaporation through the stomata of a leaf. It should also allow the simultaneous analysis of differential responses between wild-type plants and stomatal response and signaling mutants. Such a system has been developed recently and used during this thesis work (Kollist et al., 2007). The system consists of 8 stainless steel chambers, where glass covers the top of the chamber. Plants in pots are placed underneath the chambers, and spring from the bottom supports an air-tightened

connection between the plant pot and the chamber with the plant being placed inside the chamber. In the chambers, it is possible to control the environmental conditions, for example light intensity, temperature, air humidity and CO_2 concentration and these parameters are at the same time measured using a Licor gas exchange analysis device. Overall, the gas exchange system allows to measure guard cell physiology in real-time and to investigate how intact plants respond to environmental changes.

1.6. The role of ABA and biosynthesis of ABA

Previously we learned that ABA is important for stomatal closure. Still ABA also has other functions, such as regulating seed germination and root development and the promotion of leaf senescence. ABA-regulated processes are required for plant responses to drought-, osmotic-, salt-,cold-stress, and pathogen attack (Finkelstein, 2013; Leung and Giraudat, 1998; Shinozaki and Yamaguchi-Shinozaki, 2000).

For ABA synthesis (**Figure 2**) two pathways have been suggested. In the 'direct pathway,' that is mainly used by fungi, ABA is synthesized from farnesyl diphosphate (Hirai et al., 2000). In the 'indirect pathway,' ABA is synthesized through the cleavage of carotenoids in plastids (Schwartz et al., 2003). In the first step, carotenoids are converted to zeaxanthin, and Zeaxanthin is converted to violaxanthin by the zeaxanthin epoxidase enzyme (ZEP). Violaxanthin is then converted to 9-cis-violaxanthin and 9'-cis-neoxanthin, a step that is partially mediated by the enzyme ABA4. These 9-cis-epoxycarotenoids are then oxidatively cleaved by 9-cis-epoxycarotenoid dioxygenases (NCEDs) to xanthoxin (C15) and a (C25) metabolite. Xanthoxin is transported to the cytoplasm and converted to abscisic aldehyde by a short-chain dehydrogenase/reductase-like (SDR) enzyme ABA2. In the final step, the abscisic aldehyde is oxidized to ABA by ABSCISIC ALDEHYDE OXIDASE (AAO), which requires the molybdenum cofactor (MoCo) ABA3 (Schwartz et al., 2003).
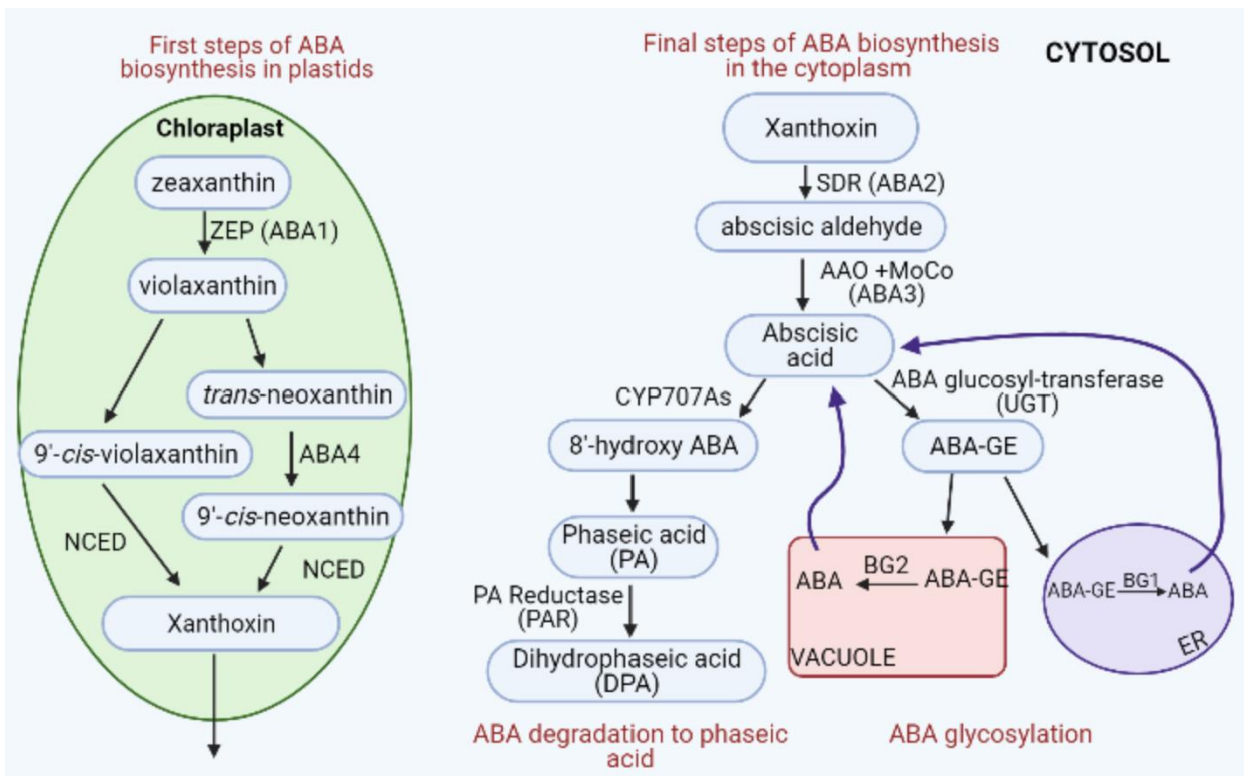
Figure 2. ABA biosynthesis in plant cells and its catabolism to phaseic acid and ABA glucose ester. The biosynthesis of ABA begins from carotenoids that are converted to zeaxanthin, followed by a conversion to violaxanthin by the zeaxanthin epoxidase enzyme (ZEP). Neoxanthin (9-cis-epoxycarotenoid) is produced from violaxanthin. It is converted to xanthoxin by an enzyme called 9-cis-epoxycarotenoid dioxygenase (NCED). Later, xanthoxin is transported to the cytoplasm and it is converted to abscisic aldehyde by ABA2, a short chain dehydrogenase/reductase-like (SDR) enzyme. The last step is catalyzed by abscisic aldehyde oxidase (AAO) to produce ABA. AAO activity requires the molybdenum cofactor (MoCo) ABA3. ABA is degraded to phasic acid (PA) by CYP707As followed by a conversion to dihydrophaseic acid (DPA) by phaseic acid reductase (PAR). ABA is also esterified to ABA glucose ester (ABA-GE) by ABA glycosyltransferases UGTs. ABA-GE is stored in the endoplasmic reticulum (ER) and the vacuole and the beta glucosidases BG1 and BG2 can convert the ABA-GE back to ABA.

Catabolism is important as synthesis. It has an essential role in ABA level regulation (**Figure 2**). Two pathways of ABA catabolism occur in Arabidopsis. 1) P-450 monooxygenase CYP707As-mediated cleave of ABA at the 8' position of the hydroxylation group, which is an unstable intermediate (8'-OH-ABA). In the next step phaseic acid (PA) is formed and converted to dihydrophaseic acid by phaseic acid reductase (PAR). 2) ABA is esterified to ABA-glucose ester (ABA-GE) by ABA glucosyltransferase enzymes (UGTs). (Finkelstein, 2013). ABA-glucose ester (ABA-GE) is an important conjugate, and ABA-GE was demonstrated that it functions as a

storage or transport form of ABA. ABA-GE is mostly stored in vacuoles and the apoplastic space, but it is also transported to the endoplasmic reticulum (ER). The β-glucosidases BG1 (BETA GLUCOSIDASE 18) and BG2 (BETA GLUCOSIDASE 33) release ABA by cleavage of ABA-GE (Xu et al., 2012). These enzymes are activated by dehydration-induced polymerization and are required for ABA recycling. The expression of *BG1* and *BG2* is shown by salinity (Lee et al., 2006).

1.7. The core ABA signaling pathway

ABA function is mediated by ABA receptors that belong to a protein family termed PYRABACTIN-RESISTANCE 1/PYRABACTIN-RESISTANCE LIKE/REGULATORY COMPONENT OF ABA RECEPTOR (PYR1/PYL/RCAR) (Ma et al., 2009; Park et al., 2009). When ABA is bound to PYR1/PYL/RCARs, they inhibit PROTEIN PHOSPHATASE TYPE 2Cs (PP2Cs), such as ABI1 (ABA INSENSITIVE 1), ABI2 (ABA INSENSITIVE 2), and HAB1 (HYPERSENSITIVE TO ABA 1), HAB2, ABA HYPERSENSITIVE GERMINATION 1(AHG1) and AHG3 (PP2CA) that functions as negative regulators of ABA signaling(Cutler et al., 2010; Ma et al., 2009; Park et al., 2009). PP2Cs, in turn, inhibit SnRK2-type protein kinases, such as SnRK2.2, SnRK2.3, and SnRK2.6/OST1. Therefore, PYR1/PYL/RCAR-ABA-mediated inhibition of PP2Cs enables the re-activation of SnRK2s that function as positive regulators of ABA signaling. In the absence of ABA, PP2Cs inactivate the SnRK2 kinases directly by dephosphorylating them (Cutler et al., 2010). Recently Raf-like MAPKKK-type protein kinases have been identified that contribute to the activation of SnRK2s in response to ABA and osmotic stress (Lin et al., 2020; Soma et al., 2020; Takahashi et al., 2020).

1.8. ABA synthesis in guard cells

It has been demonstrated that ABA is produced in the vascular bundles of plants (Kuromori et al., 2018). Expression analyzes indicated that ABA2, NCED3, and AAO3 enzymes have an essential role in ABA biosynthesis. Although while guard cells are localized on the surface layer of the plant, the vascular tissue is inside the plant leaves. When NCED3 was expressed, a change in leaf

surface temperature appeared, and probably this change happened due to the induction of stomatal closure. Therefore, ABA transport from the vasculature to guard cells must exist. On the other hand, when wild-type and *aba3-1* mutant plants were exposed to reduced relative humidity, *aba3-1* mutants wilted, while nothing happened to wild-type. But when ABA synthesis in guard cells of *aba3-1* was rescued by guard cell-specific expression of ABA3, the complemented *aba3-1* plants did not wilt in the dry air anymore, indicating that guard cells are capable of synthesizing ABA by themselves (Bauer et al., 2013). If ABA is synthesized in vascular tissues and needs to be transported to the guard cells, here we need ABA transporters which will help to close the stomata.

1.9. ABA transporters and transportation

Studying ABA in roots and leaves have led scientist to propose the "ionic trap model". It explains the movement of ABA within plants. ABA is a weak acid that can exist in an anionic (ABA$^-$) and a protonated (ABA-H) form. The pKa value of ABA is 4.7, meaning that in the apoplast, it exists as ABA-H and in the cytosol as ABA$^-$. The ionic trap model proposes that ABA-H can cross a lipid bilayer, such as the plasma membrane, but ABA$^-$ cannot. But taking into consideration that some environmental stress conditions might increase the extracellular pH value, this would lead to the decrease of membrane-permeable ABA-H. Thus, ABA transporters are needed to account for a proper ABA distribution in plants (Boursiac et al., 2013). In the "ionic trap model", another biophysical problem in ABA transport across the membrane is efflux because it explains only cellular ABA influx. Transportation of ABA into the xylem and the apoplast requires efflux transporters.

Several ABA transporters belonging to ATP-BINDING CASSETTE (ABC) transporter families were identified during the last decades. Two ABC transporters, AtABCG25 (ARABIDOPSIS THALIANA ATP-BINDING CASSETTE G25) and AtABCG40 (ARABIDOPSIS THALIANA ATP-BINDING CASSETTE G40) were involved in ABA transport and responses. AtABCG25 is expressed in the vascular tissue. Transgenic Arabidopsis plants for AtABCG25 were created, and the influence of overexpression of AtABCG25 on ABA signaling was examined. The results showed that the temperature of transgenic plant leaves was higher, and water loss was reduced compared to wild-type plants. These data indicate that AtABCG25 functions as an ABA exporter in vascular tissues and that this ABA export contributes to feeding guard cells with ABA (Kuromori et al., 2010). AtABCG40 is a plasma membrane-localized transporter for ABA. In plant

leaves, *AtABCG40* had the highest expression in guard cells. AtABCG40 cDNA was expressed in a heterologous system, a yeast strain that carries loss-of-function mutations in ABC transporters, and it showed that ABA uptake was faster. AtABCG40 is an ABA importer from the outside to the inside of the cell and functions in stomatal regulation in Arabidopsis (Kang et al., 2010). From this hypothesis, we can say that ABA can act as a mobile signal between vascular tissues and epidermal tissues, as well as guard cells and control stomatal apertures.

Another transporter, AtABCG22, has been discovered, and it is a member of the ABCG subfamily. *AtABCG22* mutant has lower leaf temperature and increased weight loss due to increased water transpiration through stomata. *ABCG22* has been expressed in guard cells and affects stomatal responses (Kuromori et al., 2011). However, whether ABCG22 transports ABA has not been proven. Furthermore, ABA controls seed germination as well. AtABCG30 and AtABCG31, as well as AtABCG25 and AtABCG40 can act as importers and exporters in Arabidopsis seeds. In Arabidopsis seeds, ABA gets released from the endosperm to the embryo. Later it can suppress the seed germination. These four transporters help to transfer ABA from the endosperm to the embryo. AtABCG25 and AtABCG31 export the ABA from the endosperm, and AtABCG30 and AtABCG40 mediate the import of ABA into the embryo (Kang et al., 2015).

After the discovery of AtABCG25 and AtABCG40 transporters that belong to the ABC transporter family, several ABA transporters were identified in different transporter families.

One of them is the ABA-IMPORTING TRANSPORTER1 (AIT1) that also functions as a low-affinity nitrate transporter NRT1.2 and belongs to the NITRATE TRANSPORTER 1/ PEPTIDE TRANSPORTER FAMILY (NPF). AIT1 (also known as NPF4.6) was identified in a yeast two-hybrid screen for proteins that enhance the interaction of PYR1 and ABI1 at very low ABA concentrations in the medium in which no interactions were usully visible. Later *ait1* mutants were compared with WT plants, and they showed reduced sensitivity to ABA during seed germination. Also, *ait1* inflorescence stems had lower surface temperature than WT plants, due to excessive water loss from open stomata. *AIT1* expression was found in inflorescence stems, leaves, and roots. It functions as an ABA importer and regulates stomatal apertures in inflorescence stems (Kanno et al., 2012). Besides AIT1/NPF4.6 also other members of the NPF family were identified as ABA transporters, such as NPF4.1/AIT3, NPF4.5/AIT2, and NPF4.2/AIT4 (Kanno et al., 2012). This two-hybrid system was further used and tested on other members of the NPF family, which led to identifying of other potential ABA importers, such as NPF1.1, NPF5.1, NPF5.2, NPF5.3, and NPF5.7 (Chiba et al., 2015).

Another transporter, DETOXIFICATION EFFLUX CARRIER 50 (DTX50), was identified as an ABA transporter. DTX50 belongs to the MULTIDRUG AND TOXIN EFFLUX TRANSPORTER (MATE) family. The *DTX50* gene is mainly expressed in vascular tissues, guard cells, and its expression is upregulated by ABA. DTX50 is primarily localized in the plasma membrane. ABA transport measurements in *Escherichia coli* and Xenopus oocytes indicated that DTX50 is an ABA exporter. *dtx50* mutant plants showed better tolerance to drought, and they were more sensitive to ABA in growth inhibition. From these, we can say that DTX50 in both vascular tissue and guard cells can export ABA (Zhang et al., 2014).

2. The aims of this thesis

Several ABA transporters were identified from different transporter families during the last decade. My main aim was to:

1. Isolate and genotype ABA transporter mutants.
2. To study the function of ABA transporters during low humidity response using the gas exchange.
3. To analyze the gene expression patterns of ABA transporters using Genevestigator.

3. Experimental Part (Materials and Methods)

3.1. Materials for molecular biology

3.1.1. gDNA isolation

liq. N_2

CTAB buffer (2% CTAB; 1% PVP 40000; 1,4 M NaCl; 100 mM Tris/HCl, pH 8.0; 20 mM EDTA, pH 8.0)

RNAseA (10 mg ml^{-1})

Chloroform

EtOH 100% (v/v)

EtOH 70% (v/v)

1x TE buffer (10 mM Tris/HCl, pH 8.0; 1 mM EDTA, pH 8.0)

2 mL tubes

Pistils

Coolable centrifuge

Chemical hood

Fridge (4 °C) and freezer (-20 °C)

3.1.2. Polymerase Chain Reaction (PCR)

10x buffer: (0.8 M Tris-HCl; 0.2 M $(NH_4)_2SO_4$)

25 mM $MgCl_2$

2 mM dNTPs

Primers (Oligonucleotides)

Fire polymerase (Solis Biodyne)

H$_2$O (autoclaved Millipore water)

1.5 mL and 2 mL tubes

PCR tubes (0.2 mL)

PCR machine (Aeris Thermal Cycler model D48)

3.1.3. Gel electrophoresis

Agarose powder (Fisher bioreagents)

0.5 TAE (Tris/Acetate/EDTA) buffer (1 M Tris; 0.055% (v/v) Acetic acid; 0.5 mM EDTA, pH 8.0)

Ethidium Bromide (EtBr) (0.5 mg mL^{-1})

DNA ladder (Thermo Scientific Gene Ruler 1kb)

Loading dye (Thermo scientific)

Erlenmeyer Flask

Gel tray (Helixx Technologies)

Comb

Microwave

Gel electrophoresis machine (GEL XL ULTRA V-2)

UV transilluminator (Cleaver Scientific Ltd)

3.1.4. DNA isolation from Agarose gels

Gel extraction kit (FAVORGEN BIOTECH CORP):

FADF buffer

Wash buffer

Elution buffer or H_2O

microcentrifugation tubes

FADF columns and Collection tubes

3.1.5. Oligonucleotides (Primers)

Table 1: Oligonucleotides used in this work. Indicated are oligo stock number, name, sequence, template, and information about what the primers were used for.

Oligo Stock	Name	Sequence	Template	Template AGI	Info
P_RW013	SALK_LB1	GTGATGGTTCACGT AGTGG	T-DNA		SALK T-DNA
P_RW014	SALK_RB	GAGACTCTAATTG GATACCGAG	T-DNA		SALK T-DNA
P_RW015	GABI_LB	CCCATTTGGACGTG AATGT	T-DNA		GABI T-DNA
P_RW016	GABI_RB	TTGTAAAACGACG GCCAGTGC	T-DNA		GABI T-DNA
P_RW035	ABCG22_5UTR_F	ggtatcgattctatatcctaag	*ABCG22*	AT5G06530	genotyping *abcg22*
P_RW036	ABCG22_In1_R	ggtaggcatgcatctttgac	*ABCG22*	AT5G06530	genotyping *abcg22*
P_RW040	ABCG25_In2_F	GGATGATAACTTG AGTGGTTC	*ABCG25*	AT1G71960	genotyping SALK_128873
P_RW041	ABCG25_Ex4_R	GAATCACATCCAA GCATTCG	*ABCG25*	AT1G71960	genotyping SALK_128873
P_RW042	ABCG31_Ex9_F	CAGTTCATTCCTGT CTCAGAC	*ABCG31*	AT2G29940	genotyping GK-064C11
P_RW043	ABCG31_Ex11_R	GATTGCTGCAGATC CGAATG	*ABCG31*	AT2G29940	genotyping GK-064C11
P_RW045	AIT1_In3_F	ctggtgttacgtcagtgtaac	*AIT1*	AT1G69850	genotyping *ait1-1*
P_RW046	AIT1_Ex4_R	GTGAGAGGACTTC CACATGG	*AIT1*	AT1G69850	genotyping *ait1-1*
P_RW047	NPF5.2_5UTR_F	AAGTGCCGACTCTC TTGAC	*NPF5.2*	AT5G46050	genotyping SALK_138430
P_RW048	NPF5.2_Ex2_R2	GACCGAGAAGAGC GTCTC	*NPF5.2*	AT5G46050	genotyping SALK_138430

3.2. Materials for Plant growth

3.2.1. Half-strength Murashige&Skoog (MS) plates

For the preparation of 400 mL 0.5 MS plates:

1.76 gL^{-1} (0.88g) MS powder

5 mM (0.43 g) MES powder

1% (w/v; 4 g) sucrose

adjust pH to 5.8 with KOH (5M)

0.8% (w/v; 3.2 g) phyto agar was added after pH adjustment.

After autoclaving, the media was poured under a sterile hood into square petri dishes, and after polymerization, the plates were stored in the fridge.

3.2.2. Soil composition

Soil composition was prepared from peat: vermiculite: water (4:2:3 respectively). The amount of soil was calculated for 42 Jyrkki pots, and each of the pots contained 250 g of soil. For gas exchange experiments, Jyrkki pots were covered with a glass plate that had a hole in the middle.

3.2.3. SNIJDER, SANYO, and long day room conditions

Plants were grown in the SNIJDER growth cabinet at 23°C in the day and 18°C in the night. Relative air humidity was 65%. The light settings for the growth chamber were 12 h light/ 12 h dark, and the light intensity was 250 µmol m^{-2}s^{-1}.

The SANYO cabinet was used to grow Arabidopsis plants on 0.5 MS plates. The light intensity was 55 µmol m^{-2}s^{-1}, the light settings for the cabinet were 12 h light/ 12 h dark, from 8:00 till 20:00 and from 20:00 till 8:00, respectively. The temperature was 23°C in the day and 19°C in the night.

Plant growth condition in the long day room had a light intensity of 150-160 µmol m^{-2}s^{-1}, light on 16 h from 8:00 till 00:00, and light off 8 hours from 00:00 till 8:00. The room temperature was 23°C.

3.2.4. Plant materials

Table 2: List of *Arabidopsis thaliana* alleles used in this work. This table illustrates the names of the ABA transporter alleles, T-DNAs, and the respective references.

Name	AGI	Allele	T-DNA	Reference
Col-0	-	-	-	-
NPF4.6/AIT1	AT1G69850	*ait1-1*	SALK_146143	(Kanno et al., 2012)
NPF5.2	AT5G46050	*npf5.2-R1*	SALK_138430	unpublished
ABCG22	AT5G06530	*abcg22-3*	SALK_024391	(Merilo et al., 2015b)
ABCG25	AT1G71960	*abcg25-R1*	SALK_128873.38.10.x	(Merilo et al., 2015b)
ABCG31	AT2G29940	*abcg31-R1*	GK-064C11	unpublished

3.2.5. Gas exchange system

The JyrkkiII system was used to run the experiments (**Figure 3**). It is a device that allows to measure 8 cuvettes (chambers) simultaneously and the chambers are made of stainless steel. On top of the chambers is a glass plate and it is assembled tightly to the chamber. There is a place to put the pot with the plant underneath the chamber. The pots are supported from the bottom side by springs. In the JyrkkiII system we can control the air humidity, the CO_2 and change the VPD by regulating the thermostat.

Figure 3. The JyrkkiII gas-exchange system. It consists of 8- cylindrical chambers, a glass on top of it covers the chamber, springs support the pots from the bottom to keep them steady, and lamps are used as light source. Plants were grown through a hole in a glass, placed under the chamber to be measured for gas-exchange experiments.

3.3. Software and Websites

3.3.1. Software

Biorender: used for making the figures (https://biorender.com/).

Fiji: used for leaf area calculations (https://imagej.net/Welcome).

Genevestigator: used for transcript analysis (https://genevestigator.com/).

Microsoft Excel: used for data analysis.

Microsoft Powerpoint: used for making the figures.

SnapGene: used for molecular biology analysis, DNA sequence analysis (https://www.snapgene.com/).

3.3.2. Websites

Google Scholar: used for article/paper search (https://scholar.google.de/w)

PUBMED: used for article/paper search (https://pubmed.ncbi.nlm.nih.gov/)

Research gate: used for article/paper search (https://www.researchgate.net/)

Tair: used for BLAST and to find dataset about Arabidopsis (https://www.arabidopsis.org/)

3.4. Methods

3.4.1. gDNA isolation

- Cut 1 leaf from the plant and put it into a 2 mL tube. Immediately put the tube inside liq. N_2.
- Take the tube out of liq. N_2 and crush the leaf with a precooled pistil.
- Add 600 µL of CTAB DNA extract buffer and vortex it until the sample is solubilized.
- Incubate at 65°C for 1 hour and invert the tube 2 times at 20-minute intervals.
- Let the sample cool down for 10 minutes. Thaw RNAseA (10 mg mL^{-1}) on ice.
- Add 1 µL RNAseA to the sample and mix by inverting the tube.
- Incubate the sample for 1 hour at 37°C.
- Under the hood, add 600 µL Chloroform, mix gently by inverting the tube and spin for 10 minutes at 5000 rpm and room temperature.
- Under the hood, transfer the polar phase (500 µL) from the sample to a new 2 mL tube.
- Add 2.5x volume (1250 µL) of -20°C EtOH (100%; v/v) and mix the tube by inverting.
- Incubate the tube at -20°C for 30 minutes.
- Precipitate gDNA by centrifugation at full speed and 4°C for 30 minutes.
- Discard the supernatant and add 500 µL of -20°C EtOH (70%; v/v).
- Spin the sample at full speed for 4°C for 10 minutes and discard the supernatant.
- Dry the DNA pellet at 55°C in a thermoblock.
- Resuspend DNA in 60 µL of TE (Tris-EDTA) buffer.
- Incubate DNA overnight at 4°C and store it at 4°C in the fridge.

3.4.2. PCR reaction

Table 3: Reagents used for PCR reactions.

Component	Volume
10x buffer	2.0 µL
25 mM MgCl$_2$	2.0 µL
2 mM dNTPs	2.0 µL
10 µM Primer 1	0.4 µL
10 µM Primer 2	0.4 µL
Fire polymerase	0.2 µL
H$_2$O	12 µL
gDNA template	1 µL
Final volume	20 µL

For multiple samples, a master mix was prepared in a 2 mL tube. Before the master mix was distributed to PCR tubes (20 µL) it was mixed by pipetting. Before the PCR reaction, the samples in the PCR strip were spun briefly in a small table centrifuge before they were placed into the PCR machine.

3.4.3. PCR machine settings

Table 4: Standard program for PCR reactions.

PCR step	Temperature	Duration
1) Initial denaturation	95°C	5 minutes
2) Denaturation	95°C	30 seconds
3) Annealing	55°C	30-45 seconds
4) Extension	72°C	60 seconds per 1000 bp
5) Cycle 35 times steps 2 to 4		
6) Final extension	72°C	5 minutes
7) Cooling	8°C	∞ - infinity

When the PCR machine stopped, the samples were ready to be loaded on an agarose gel.

3.4.4. Agarose gel preparation

- The size of the gel depended on the amount of the samples and loading volume. 1% (w/v) of agarose in 0.5x TAE buffer was used for standard agarose gel preparations.
- Weight agarose powder on a fine balance.
- Transfer agarose powder into an Erlenmeyer flask.
- Add desired amount of 0.5x TAE buffer to obtain an 1% (w/v) agarose gel.
- Heat solution in a microwave until agarose appears completely dissolved.
- Add Ethidium Bromide (EtBr) (0.5 mg/mL) 1 drop per 50 mL solution.
- Tape an agarose gel tray to avoid leakage, place it into an agarose gel pouring system and add a gel pocket comb.
- Pour the hot agarose solution into the gel pouring system, remove air bubbles and let the gel solidify for at least 40 minutes.

3.4.5. Agarose gel electrophoresis

- Add 2 µL DNA loading dye to the PCR samples using a repetition pipette.
- Place the solidified agarose gel with tray, but without comb into the gel electrophoresis system.
- Make sure that the agarose gel is completely covered in 0.5x TAE buffer.
- Mix each PCR sample by brief pipetting and load 10-20 µL of the reaction into an agarose gel pocket.
- Load the first and the last agarose gel pocket with 7 µL of 1 kb DNA ladder.
- Run small gels (60 mL) at 100 V and large gels (120 mL) at 135 V for 25-30 minutes.

3.4.6. Analysis of agarose gels and isolation of DNA fragments from agarose gels

- Remove the agarose gel from the gel electrophoresis system.
- Place the gel without tray onto the UV transilluminator.
- Under white light, align the agarose gel so that it fits into the image acquisition area of the camera and adjust the magnification of the camera.
- Turn off the white light, turn on the UV light and acquire an image.
- For DNA fragment isolation, cut the desired band from the gel using a scalpel blade and place it into a 2 mL tube. Make sure that the eyes are protected by the plexiglass UV shield.

3.4.7. DNA purification from an agarose gel

- Add 500 µL of FADF buffer to the sample and vortex it.
- Incubate at 55°C for 5-10 minutes until gel is completely dissolved.
- Cool down the sample to room temperature and place a FADF column into a Collection tube.
- Transfer 800 µL of the sample to the FADF column, and centrifuge at 11000 x g for 30 seconds. Discard the flow-through.
- Add 750 µL of wash buffer to the FADF column and centrifuge at 11000 x g for 30 seconds. Discard the flow-through.
- Centrifuge at full speed for 3 minutes to dry the column matrix. Prepare a 1.5 mL tube and transfer the FADF column into it.
- Add 30 µL of H_2O to the center of the FADF column.
- Centrifuge at 13200 x g for 1 minute to elute the DNA.
- Pipet the elution back onto the FADF column and repeat the centrifugation step.

3.4.8. Sequencing of PCR fragments

- Prepare PCR tubes and label them accordingly.
- Add 5.7 µL of purified PCR product to the PCR tubes.
- Prepare another tube and add 5 µL of diluted primers.

- Check that the sample names match the template names on the order form.
- Put the order form and tubes into the sample submission bag.
- Ship the samples for sequencing.
- For sequencing analysis please refer to 3.6.1

3.5. Plant work

3.5.1. Seed sterilization, sowing, plant growth and seed harvesting

- Add Arabidopsis seeds into a 2 mL tube. Protect the tube label with a transparent tape.
- Add to the tube 1 mL of 70% (v/v) EtOH under the laminar hood.
- Rotate the tube for 10-15 minutes over-head.
- Let the seeds settle down and removed the EtOH from the tube by pipetting.
- Add 1 mL 100% (v/v) EtOH and invert the tube 30 times overhead for seed washing.
- Repeat the washing step three more times.
- Dry the seeds under the laminar hood for ca. 2.5 hours.
- Transfer a 0.5 MS plate under the laminar hood, open the lid for 1 hour for drying.
- Transfer dry seeds onto a sterile paper.
- Using sterile toothpicks place the seeds one-by-one onto the 0.5 MS plate.
- Close the plate with micropore tape.
- Wrap the plate in aluminum foil.
- Stratify the sowed seeds in the fridge for 4 days.
- Removed the aluminum foil and put the plate into the SANYO cabinet.
- Grow the plants for 6 days in the SANYO cabinet.
- Prepare pots with soil.
- Using forceps, transfer single seedlings into a plant pot and make sure that the root is embedded in the soil by adding water to the seedling.
- Grow plants in the long-day room and water them 1-2 times per week.
- When plants start bolting, encircle them with a plastic sheet to avoid cross contamination of seeds.
- After 8 weeks, stop watering the plants for 2 weeks.
- Cut the shoot from the dried plants into pieces and place them onto a paper.
- Using gentle pressure, retrieve the seeds from the siliques.

- Filter the seeds from plant debris onto a new paper by using a double metal sieve.
- Transfer rolling seeds to a new paper and into a 1.5 mL tube.

3.5.2. Plant growth for gas-exchange analysis

- Transferred approximately 50 µL of seeds into a 2 mL tube.
- Add 500 µL of sterile water and mixed well.
- Transfer the tubes with seeds into a cardboard box and stratify the seeds for 3 days in the fridge.
- Prepare Jyrkki pots. Add 250 g of soil mixture to the pot and cover it with a glass plate that contains a hole in the middle. Make sure that the area in the middle of the pot with the glass hole is completely underlaid with soil.
- Using a cut yellow pipet tip, mix the stratified seeds in water and add ca. 20 µL of the seed suspension onto the soil beneath the glass hole of the Jyrkki pot.
- Cover the sowed seeds with a small plastic petri dish.
- Transfer the Jyrkki pots to the SNIJDER growth cabinet and water the plants once per week by bottom watering.
- After one week, remove the plastic lids and single the plants in each pot.
- A few days before the gas exchange measurements use paraffin wax to tighten the glass hole through which the plant grew so that no air exchange is possible between both sides of the glass plate.

3.5.3. Gas exchange measurements

- Check water levels in water thermostats and air pre-humidifier.
- Remove excess water from the humidifier thermostat drainage port and add 20-25 mL demineralized water.
- Turn on the thermostats for temperature (22 °C) and humidity control (between 15.5 and 16.5 °C).
- Open the air flow valve and turn on the air flow pump.

- Turn on the lights and set the light intensity to 150 µmol $m^{-2}s^{-1}$. For light intensity measurements use a quantum meter.
- Remove air bubbles from the system.
- Turn on the LICOR device and its computer connection system.
- Turn on the computer and start the Ozone software.
- Rename the data output file.
- Select the chambers to be measured and immediately turn on the pump to the LICOR device.
- Set the chamber measurement time to 30 seconds reference and 30 seconds sample measurements.
- Select the plants to be measured and acquire a picture of each along a mm scale to enable leaf area measurements.
- Transfer each plant into a measurement cuvette and make sure that no air is leaking.
- Adjust the humidifier thermostat temperature to control air humidity in the cuvettes. The air humidity should be ca. 65%.
- Adjust the system pressure to 41 mmHg.
- After stabilization of the system, restart the ozone software and run the VPD experiment protocol: 1 hour baseline recording, 3 hours high VPD (ca. 35 % relative humidity) and 3 hours recovery at ca. 65% relative humidity.
- During the low air humidity treatment, change the gas flow from the humidifier thermostat to a gas flow through an ice cooled copper spiral and adjust the system pressure to 41 mmHg.

3.6. Office work

3.6.1. Making the genomic maps using SnapGene

- Copy AGI number and make a search on the TAIR website.
- Copy the genomic DNA sequence from TAIR to SnapGene.
- Find the sequences for 5'- and 3'-UTRs, primers, exons and introns and generate features for each one.
- To find the exact T-DNA location (Left border and Right border), add the sequence from the annotated T-DNA insertion and from the respective sequencing results to the TAIR website,

choose settings for BLAST program and dataset (BLASTN, Genomic locus sequences) and Run BLAST.

- Select 20 bp from the start of the BLAST result, make a sequence search in SnapGene and mark the identified sequence as a feature.

3.6.2. Leaf area measurements using ImageJ (Fiji)

- Plant pictures of were taken using a Sony DSC-RX100 camera. For image calibration, a mm paper was used alongside with the plants.
- Acquired images were downloaded from the server and renamed according to the genotype and plant number.
- Images were opened in Fiji and calibrated according to the mm paper.
- After cropping the pictures to a smaller size, a color thresholding was applied to select the plant leaf area. Invisible plant parts were manually added to the leaf area based on educated guess.
- Leaf areas were measured based on the selected regions.

3.6.3. Gas exchange data analyses using Excel

- Open ozone VPD experiment text file and replace all comas (,) with dots (.), and save.
- Create a new excel file.
- Transfer text file to excel and save as excel.xlsx.
- Delete the first 5 rows (zeroes), and insert a new column, label it as "time and min".
- Insert timescale from -60 to 360 min.
- Select complete dataset and sort the data according to the sample name (cuvette number).
- Make a new Allele column and insert the allele names.
- Separate the sample data by two new rows.

- Open the Gas Exchange Template file. All formulas were calculated in this template file.

- Copy all headers and formulas from the template file and paste them into the excel sheet above each data set.
- Correct the values for the leaf areas and propagate the formulas to the entire dataset.
- Select time, corr stomatal conductance and relative air humidity columns to generate charts for each allele.

- Create a new excel file.
- Copy for each genotype the allele, time, corr. stomatal conductance and relative air humidity column data and paste them into a genotype-specific sheet.
- Paste the data of experiments 1, 2, 3, and 5 besides each other, and below each other. From the below each other data generate a scatter plot for each genotype.
- Perform the calculations mentioned below for each experiment and genotype.
- For the calculation of the basal corr. stomatal conductance, calculate the average of the last 3 data points before the high VPD treatment.
- For the calculation of the initial high VPD response rate, subtract the average of the last 3 data points before the high VPD treatment from the corr. stomatal conductance at 8-12 minutes after the treatment and divide the result by the respective time interval.
- For the calculation of the corr. stomatal conductance change after 3 h VPD treatment, calculate the average of the last 3 data points of the high VPD response minus the average of the last 3 data points before the high VPD treatment.
- For the calculation of the initial high VPD recovery rate, subtract the corr. stomatal conductance at 8-12 min after the change to 65% relative humidity from the average of the last 3 data points of the high VPD response and divide the result by the respective time interval.
- For the calculation of the corr. stomatal conductance change after 3 h recovery from high VPD, calculate the average of the last 3 data points of the entire experiment minus the average of the last 3 data points of the high VPD response.
- Copy and paste special (values/transpose) the results into a new table.
- Calculate the averages and standard deviations among the respective experiments.
- Generate genotype sorted data tables, paste them into a new 'summary' sheet and generate bar graphs with indicated standard deviations.

3.6.4. Genevestigator analyses

- Choose the data collection. Select by experiments or samples.
- Create a folder containing the default Arabidopsis data collection.
- Enter genes of interest and select the entire gene set from the collection.
- Analyze the gene expression patterns using the condition search tools Anatomy, Perturbation and Development.
- Sort the data according to Log2 ratio, Fold change (if only one gene is selected), Pi -score (for sorting combined results of multiple genes), and P-value.
- Filter by Fold-change and P-value and selected the most strongly regulated conditions.
- Export the data to an excel sheet and save the workspace.
- Check the anatomy and development of the genes and selected the most important datasets.
- Export the data as .pdf files and save the workspace.

3.6.5. Preparation of figures using Biorender

For figure preparations the Biorender website was used. This website had a lot of opportunities and provided tools to make the figures from scratch.

4. Results and Discussion

4.1. Isolation and genotyping of ABA transporter mutants

To genotype ABA transporter mutants we isolated genomic DNA, performed PCR analyses, and sequenced the PCR products to correctly annotate the respective T-DNA insertion sites in a given T-DNA mutant allele. For further information about the procedures see **3.4.1** to **3.4.8**. The genotyping analyses of the ABA transporter mutants and the respective genomic DNA maps of the ABA transporter genes are shown in **Figure 4** (ABCG-type transporters) and **Figure 5** (NPF-type transporters). For the ABCG transporters, *ABCG22* (AT5G06530)*, ABCG25* (AT1G71960) and *ABCG31* (AT2G29940)*,* we used the alleles *abcg22-3* (SALK_024391) (Merilo et al., 2015)*, abcg25-R1* (SALK_128873.38.10.x) (Merilo et al., 2015)*,* and *abcg31-R1* (GK-064C11)*,* respectively. Their T-DNA insertions are located for *abcg22-3* in intron 1, for *abcg25-R1* in exon 3, and for *abcg31-R1* in exon 10 (**Figure 4**). For the NPF transporters, *NPF4.6/AIT1* (AT1G69850) and *NPF5.2* (AT5G46050) we used the alleles *ait1-1* (SALK_146143) (Kanno et al., 2012) and *npf5.2-R1* (SALK_138430)*.* The T-DNA insertion for *ait1-1* is located in exon 4 and for *npf5.2-R1* in exon 1 (**Figure 5**). Altogether, we could faithfully confirm the T-DNA insertion locations and isolate homozygous T-DNA insertion alleles for all investigated transporter genes (**Figure 4** and **Figure 5**). The *npf5-2-R1* allele has not been used before, whereas in previous research another mutant allele of *ABCG31* was used (Kang et al., 2015). In our study we choose the above-mentioned alleles because their T-DNA insertions are located more upstream in an exon, and not in an intron.
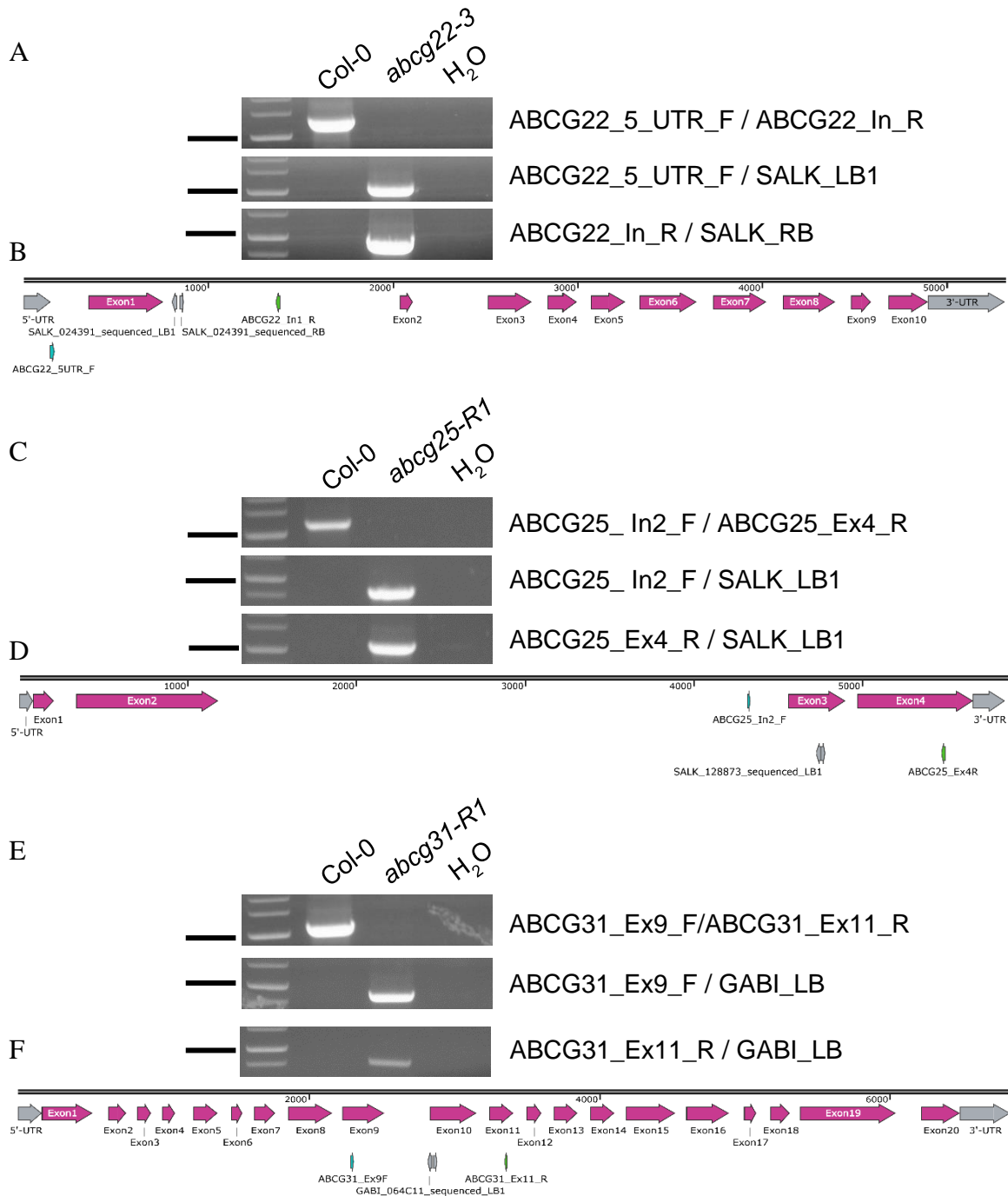
Figure 4. Genotyping and genomic maps of ABCG-type transporters. (A,C,E) Genotyping PCR results of Col-0 wild type and *abcg* mutant alleles using the indicated primer combinations. The black lines on the left indicate the 1 kb band of the DNA ladder. (B,D,F) Genomic maps of the used *ABCG* transporter genes indicating 5'- and 3'-untranslated regions (UTRs; grey), exons (magenta), the location of the respective primer-binding sites and the confirmed T-DNA insertions with annotated left border (LB) and right border (RB) T-DNA orientation.
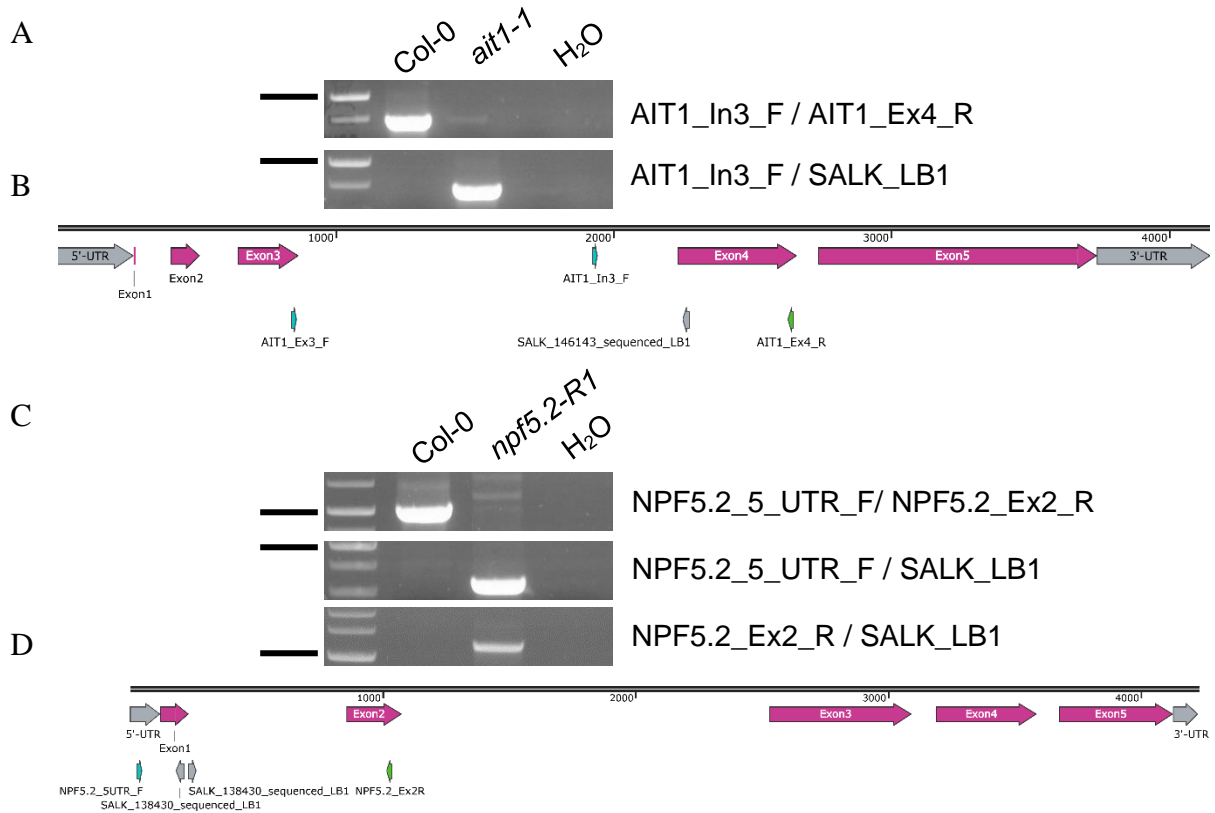
Figure 5. Genotyping and genomic maps of NPF-type transporters. (A,C) Genotyping PCR results of Col-0 wild type and *npf* mutant alleles using the indicated primer combinations. The black lines on the left indicate the 1 kb band of the DNA ladder. (B,D) Genomic maps of the used *NPF*-type transporter genes indicating 5'- and 3'-untranslated regions (UTRs; grey), exons (magenta), the location of the respective primer-binding sites and the confirmed T-DNA insertions with annotated left border (LB) T-DNA orientation.

4.2. VPD response analysis using gas exchange of ABA transporter mutants compared to Col-0 wild type

To test if the above isolated ABCG- and NPF-type transporters have an altered response to high VPD (a change from 70% relative humidity (RH) to ca. 35% RH), or an altered recovery response from low RH, we performed gas-exchange analyses using the JyrkkiII system (**Figure 3**). For this, we selected one plant of each genotype and placed them into the JyrkkiII system. Then we recorded the basal stomatal conductance for 1 hour at ca. 70% RH, followed by a 3-hour treatment with low humidity (ca. 35% RH). For very large plants, the JyrkkiII system could reduce the RH only to ca. 50%. Finally, we recorded the recovery of those plants after a change of the RH back to ca. 70% for 3 hours. Overall, we did four experimental replicates for all genotypes and the results of the corrected stomatal conductance change (blue) and RH change (orange) are shown in **Figure 6**. We observed that all genotypes responded to low humidity. Except of *abcg22-3*, all other alleles responded similar compared to wildtype. *abcg22-3* appeared to respond slower compared to Col-0 wild-type (**Figure 6**).
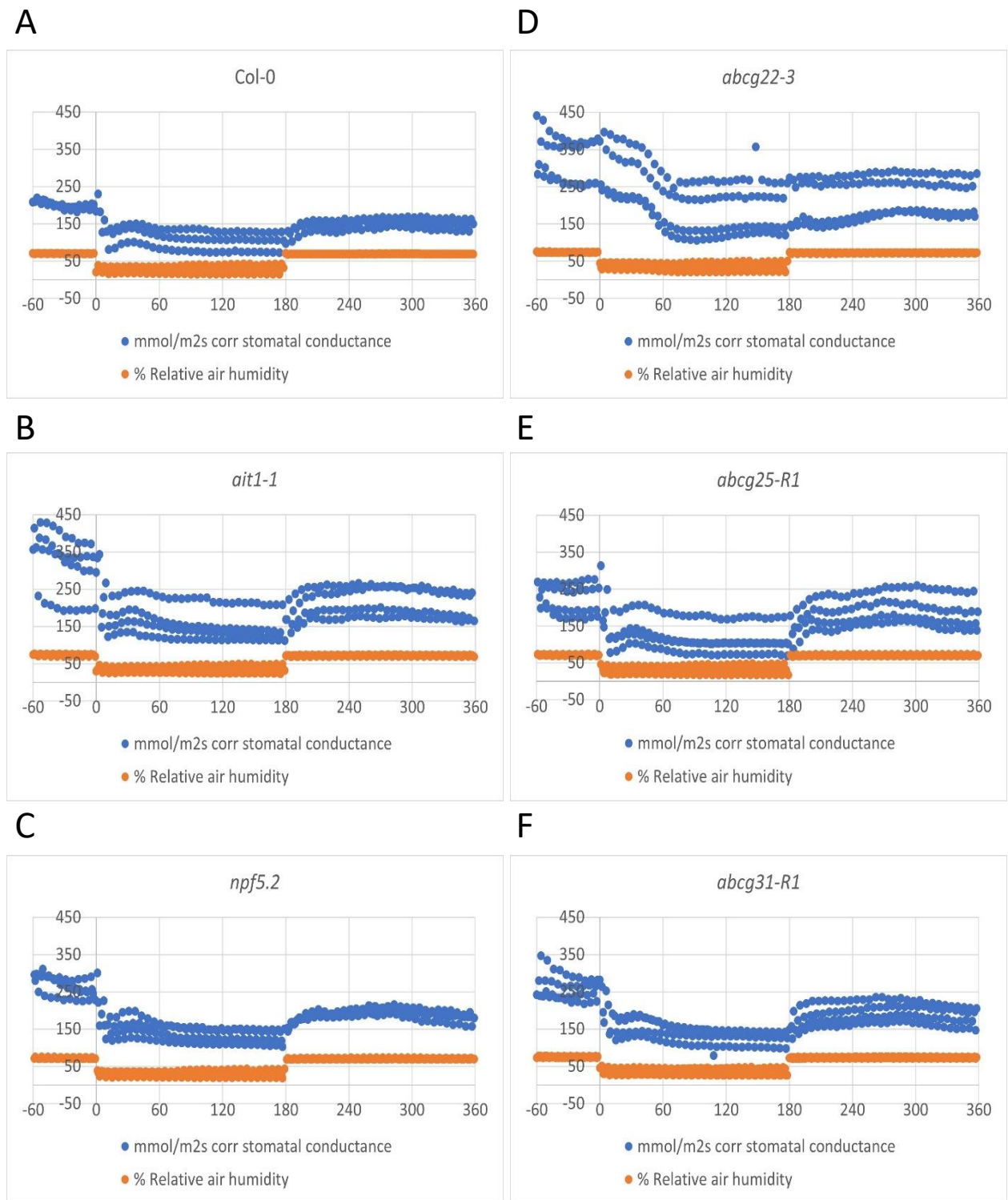
Figure 6. VPD response analysis of ABA transporter mutants using gas exchange. Time-dependent analyses of the corrected stomatal conductance (blue) and the relative air humidity (RH) (n = 4 experimental replicates) of **A)** Col-0, **B)** *ait1-1*, **C)** *npf5.2-R1*, **D)** *abcg22-3*, **E)** *abcg25-R1* and **F)** *abcg31-R1* in response to high VPD (a change from ca. 70% RH to ca. 35% RH) applied at time-point 0 minutes. After 3 hours of high VPD treatment, the RH was changed back to ca. 70% RH and the plant recovery was analyzed for additional 3 hours. All genotypes responded to low humidity, except of *abcg22-3*, which responded slower compared to Col-0 wild type and the other alleles.

From the data in **Figure 6** we calculated additional parameters, such as the basal stomatal conductance before the high VPD treatment, the stomatal conductance change after 3 hours of high VPD treatment, the stomatal conductance change after 3 hours of recovery from the high VPD treatment, the initial VPD response rate, and VPD recovery rate. The corresponding data are presented in **Figure 7**. What we can see is that *ait1-1* and *abcg22-3* have higher basal stomatal conductance compared to Col-0 wild type (**Figure 7A**). For the VPD response change (**Figure 7B**), all alleles showed a higher response change compared to Col-0 wild type. *ait1-1* showed the strongest response. For the VPD recovery change (**Figure 7C**), *abcg25-R1* showed the highest recovery change, while *abcg22-3* had the lowest recovery change. The other alleles were comparable to Col-0 wild type. *abcg22-3* showed the lowest VPD response rate (**Figure 7D**), which was also clearly visible in the temporal analyses in **Figure 6**. *ait1-1*, *npf5.2*, and *abcg25-R1* responded faster than Col-0 wild type. As for the VPD response rate, we obtained similar results for the VPD recovery rate (**Figure 7E**). Here, *abcg22-3* recovered slower compared to Col-0 wild type, while the other mutant alleles recovered faster.

High VPD response analyses using mutant alleles such as *ait1-1*, *abcg22-3* and *abcg25-R1* have been performed before ((Merilo et al., 2015a)). As our results indicate that *abcg22-3* has the strongest impairment in the high VPD response (**Figure 6** and *Figure 7*), the same phenotype was observed before (Merilo et al., 2015). Overall, we did not identify any additional ABA transporter genes that have a clear function in the high VPD response.
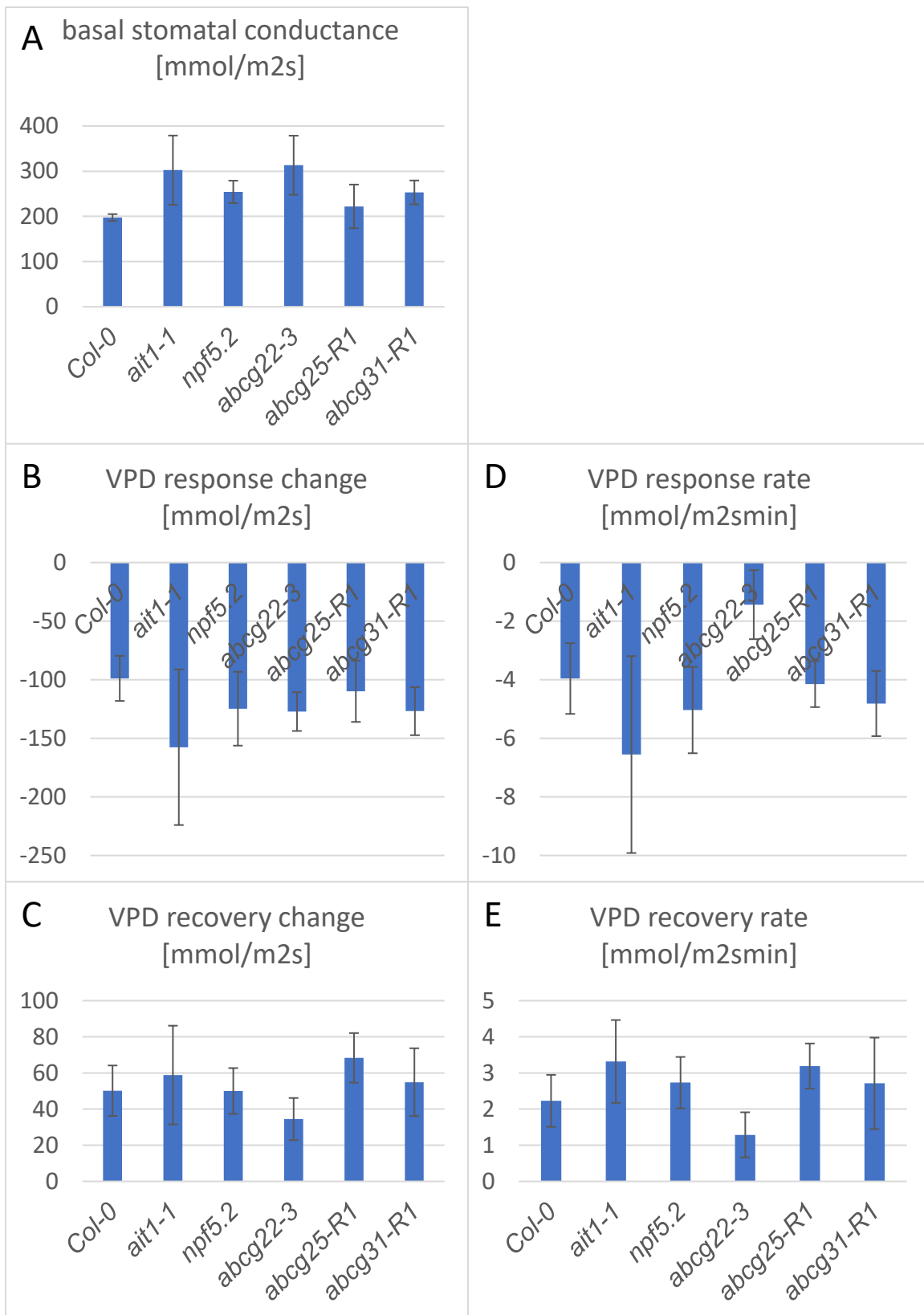
Figure 7. Stomatal response parameters of ABA transporter mutants compared to Col-0 wild type. A) Basal stomatal conductance, before treatment. **B)** VPD response

change, is the difference between 3 hours after treatment and basal conductance. **C)** VPD recovery change, is the difference between 3 hours recovery and end of the treatment. **D)** VPD response rate, is the initial rate of stomatal conductance change in response to the treatment. **E)** VPD recovery rate is the initial rate of stomatal conductance change after release from the treatment. Data derived from experiments in **Figure 6** and are represented as means ± standard deviation of n = 4 experimental replicates.

In my analyses, I tested only five ABA transporter genes for their function in the high VPD response. However, several other ABA transporters have been identified (Zhang et al., 2014; Chiba et al., 2015; Kang et al., 2015). To develop a hypothesis about the potential function of these ABA transporters, it is always good to check their expression patterns. Maybe some transporters are expressed more strongly in seeds, others more strongly in guard cells or the vasculature. For this, gene expression analyses using Genevestigator are useful.

4.3. Gene expression analysis of ABA transporters using Genevestigator.

We looked closely to the expression site of the ABA transporters using Genevestigator. From the Arabidopsis microarray analysis data collection, we selected the ABA transporter genes and analyzed their expression patterns using the anatomy, perturbation, and development tools in Genevestigator. The development tool generates a heat-map showing ten developmental stages: germinated seeds, young seedling, young rosette, developed rosette, bolting stage, young flower, developed flower, flowers and siliques, mature siliques, and seeds, respectively (**Figure 8.**). ABA transporters that expressed in all developmental stages are *NPF3.1*, *NPF4.2*, *NPF4.5*, *NPF5.3*, *NPF5.7* and *ABCG25*. Strongly expressed ABA transporter genes in flowers and siliques are *NPF4.1*, *NPF4.5*, and *NPF5.1*, while *NPF8.2*, *ABCG25* and *ABCG31* are expressed slightly less. Strongly expressed transporters during seeds germination are *ABCG25* and *ABCG30*. *NPF5.2*, *NPF4.7*, *ABCG40* and *AT5G52050* (*DTX50*) had almost no expression in any developmental stage (**Figure 8. Genevestigator analysis of ABA transporter expression using the development tool.** In the color scale bar, white indicates low or no expression and blue indicates strong expression. The developmental stages show the steps of the growth. The data for each ABA transporter gene were calculated from the average number of samples.).

Figure 8. Genevestigator analysis of ABA transporter expression using the development tool. In the color scale bar, white indicates low or no expression and blue indicates strong expression. The developmental stages show the steps of the growth. The data for each ABA transporter gene were calculated from the average number of samples.
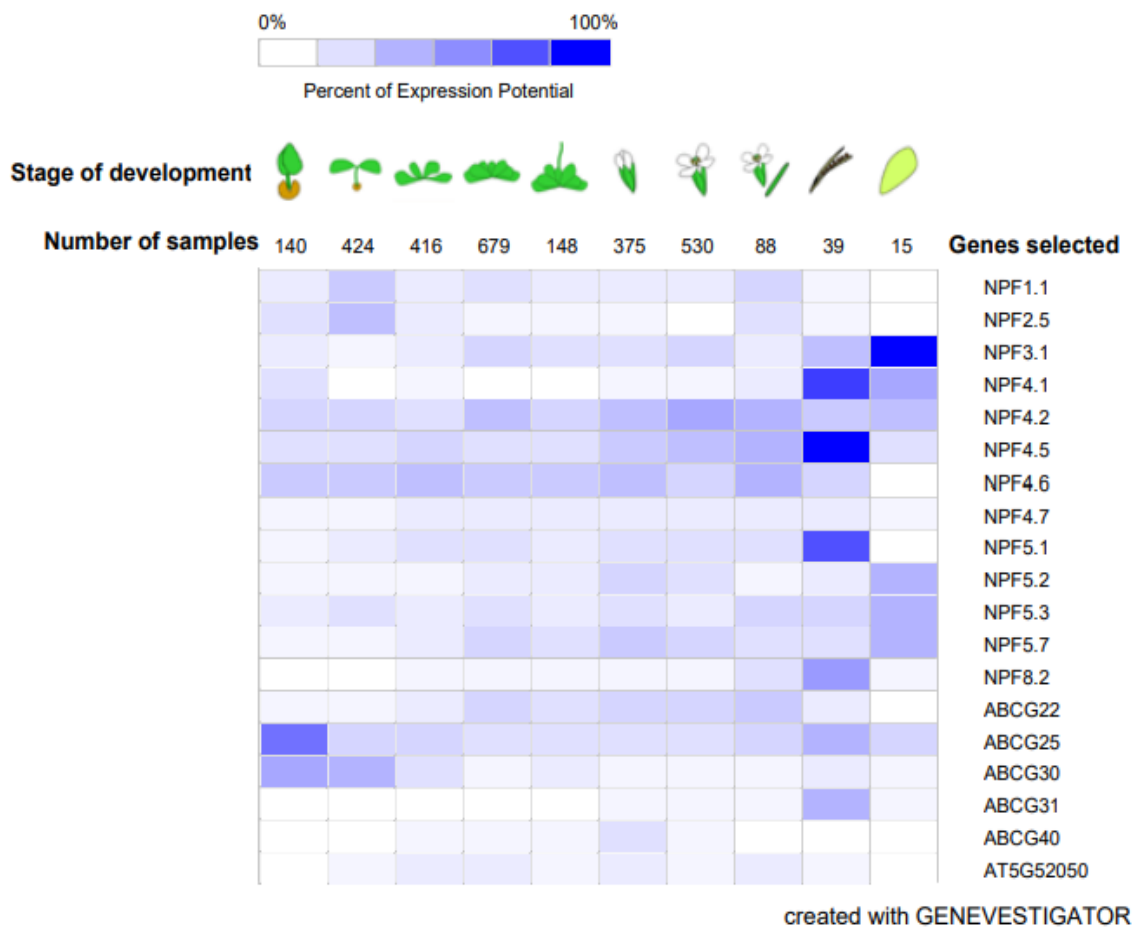
From the anatomy data, we condensed the important stages of plant development and created a table to illustrate the results (**Table 5:**). This table provides information about the developmental stage, together with tissue- and cell-specific expression patterns of ABA transporters. In **Table 5:** , we marked in yellow color the most expressed transporters. Highly expressed transporters in guard cells are *NPF1.1*, *NPF4.6/AIT1*, *NPF5.1*, *NPF5.2*, *NPF5.7*, *ABCG22*, *ABCG31* and *ABCG40*, while *NPF2.5* and *NPF3.1* are weakly expressed. In the seed stage, *NPF3.1*, *NPF4.1/AIT3*, *NPF4.5/AIT2*, *NPF4.6/AIT1* and *ABCG25* are the ones that show the highest

expression levels compared to others. In the flower stage *ABCG31* shows an extremely high expression, while in the stele there is only 1 transporter *NPF4.6/AIT1* which is strongly expressed.

Table 5: Tissue- and cell-specific expression levels of ABA transporters. Shown are the ABA transporter names, their respective AGI code, and the average expression levels of the ABA transporters in the indicated tissues and cell types. High levels of gene expression are marked in yellow.

Name	AGI	Rosette	Primary root	Lateral root	Root tip	Flo-wer	Seed	Endo-sperm	Infloure-scence stem	Stele	Guard Cell
NPF1.1	AT3G16180	2860	9202	6135	7595	1535	1680	849	9334	803	3658
NPF2.5	AT3G45710	242	5815	11805	3626	532	303	374	1338	736	225
NPF3.1	AT1G68570	6626	456	842	391	10590	5873	679	4949	1497	399
NPF4.1/AIT3	AT3G25260	554	434	402	413	789	6414	7781	558	1420	538
NPF4.2/AIT4	AT3G25280	366	287	279	283	458	661	1970	377	779	570
NPF4.5/AIT2	AT1G27040	515	433	651	405	1319	3483	12046	558	655	1054
NPF4.6/AIT1	AT1G69850	4283	2875	3533	1634	1301	2522	1590	4123	4640	20290
NPF4.7	AT5G62730	536	291	277	290	3007	360	287	435	751	516
NPF5.1	AT2G40460	1898	731	1908	331	1612	2084	585	2093	626	7834
NPF5.2	AT5G46050	3132	1582	1400	1002	1117	1782	394	721	594	13381
NPF5.3	AT5G46040	252	524	466	343	461	658	911	273	598	1723
NPF5.7	AT3G53960	3299	377	430	311	1939	1054	424	3709	783	5756
NPF8.2	AT5G01180	493	273	244	268	8514	1877	2103	389	711	2180
ABCG22	AT5G06530	7607	1044	696	524	3268	1896	486	5436	651	50290
ABCG25	AT1G71960	969	1246	963	599	977	2508	4056	1983	888	1869
ABCG30	AT4G15230	567	3813	3194	3319	700	1495	2372	891	717	585
ABCG31	AT2G29940	409	252	229	244	72558	1155	538	446	711	19645
ABCG40	AT1G15520	3906	646	568	560	1653	366	290	638	1033	6998
DTX50	AT5G52050	2116	818	806	603	760	592	627	639	1062	867

In general, *NPF1.1*, *NPF4.6/AIT1*, *ABCG22* and *ABCG30* showed a strong expression in almost all developmental stages. *NPF4.2/AIT4*, *NPF4.7*, *NPF5.1*, *NPF5.3*, *NPF8.2* and *DTX50* were the weakest expressed transporters. These transporters were either weakly expressed in any developmental stage or exhibited a very specific and local expression pattern. In comparison, other gene expression analyses in Arabidopsis reported a high expression of *NPF4.6/AIT1*, *ABCG22*, *ABCG25* and *ABCG31* in guard cells (Merilo et al., 2015b). However, only gene expression of ABCG25 showed an increased expression in response to ABA or low humidity (Merilo et al., 2015b). Compared to (Merilo et al., 2015b), our analyses indicate that ABCG25 was one of the lowest expressed genes in guard cell, while ABCG22, ABCG31, and NPF4.6/AIT1 showed the strongest expression, similar as reported by (Merilo et al., 2015b).
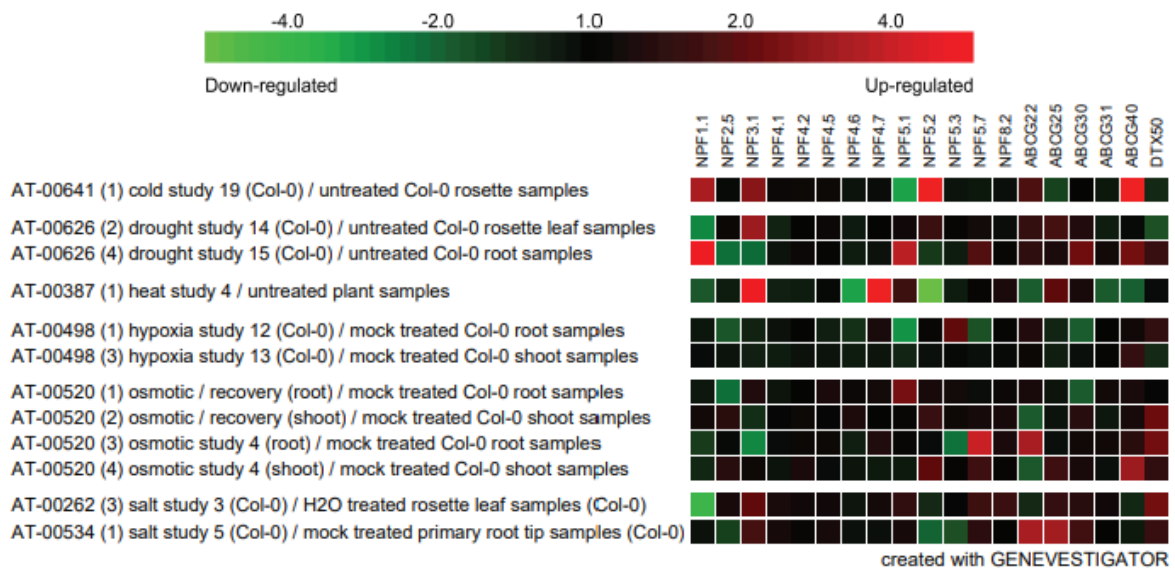
Figure 9. Genevestigator ABA transporter expression analyses in response to abiotic stresses. The text on the left indicates the respective abiotic stresses and the investigated Arabidopsis plant tissues. The heat map on the right indicates the ABA transporter gene expression changes in response to the abiotic stress, with down-regulated genes colored in green and up-regulated genes colored in red.

ABA levels in plants are increasing due to abiotic stress, and high levels of ABA can lead to an adaptation of plants to various abiotic stresses. Gene expression analyses of ABA transporter genes in response to abiotic stresses (**Figure 9. *Genevestigator ABA transporter expression analyses in response to abiotic stresses. The text on the left indicates the respective abiotic stresses and the investigated Arabidopsis plant tissues. The heat map on the right indicates the ABA transporter gene expression changes in response to the abiotic stress, with down-regulated genes colored in green and up-regulated genes colored in red.*) indicate that *NPF1.1*, *NPF3.1*, *NPF5.2*, and *ABCG40* are up-regulated, while *NPF5.1* is down-regulated in response to cold stress. In response to drought stress, *NPF1.1* and *NPF5.1* are up-regulated in roots and *NPF3.1* in rosettes, while *NPF1.1* and *DTX50* are down-regulated in rosettes, and *NPF2.5* and *NPF3.1* are down-regulated in roots. In response to heat stress, *NPF3.1* and *NPF4.7* are up-regulated, while *NPF4.6* and *NPF5.2* are strongly down-regulated. Hypoxia had almost no effect on ABA transporter gene expression. Only *NPF5.1* is strongly down-regulated. During osmotic stress, *NPF5.7*, *ABCG22* and *DTX50* are up-regulated in roots and *ABCG40* is up-regulated in shoots, while *NPF3.1* and *NPF5.3* are down-regulated in roots and *ABCG22* is down-regulated in shoots. During recovery

from osmotic stress, *NPF5.1* is up-regulated in roots and *DTX50* is up-regulated in roots, while *NPF5.2* and *ABCG30* are down-regulated in roots and *ABCG22* is down-regulated in shoots. Finally, in response to salt stress, *ABCG22* and *ABCG25* are up-regulated in roots, while *NPF1.1* is down-regulated in rosettes and *NPF5.2* is down-regulated in roots (**Figure 9. *Genevestigator ABA transporter expression analyses in response to abiotic stresses.* The text on the left indicates the respective abiotic stresses and the investigated Arabidopsis plant tissues. The heat map on the right indicates the ABA transporter gene expression changes in response to the abiotic stress, with down-regulated genes colored in green and up-regulated genes colored in red.**). From **Figure 9. *Genevestigator ABA transporter expression analyses in response to abiotic stresses.* The text on the left indicates the respective abiotic stresses and the investigated Arabidopsis plant tissues. The heat map on the right indicates the ABA transporter gene expression changes in response to the abiotic stress, with down-regulated genes colored in green and up-regulated genes colored in red.** we can summarize that gene expression of *NPF1.1*, *NPF3.1*, *NPF5.1*, *NPF5.2* and *ABCG22* is altered in response to almost all investigated abiotic stresses, while *NPF4.1*, *NPF4.2*, *NPF4.5* and *NPF8.2* did not change their expression levels in response to any abiotic stress.

Gene expression analyses of ABA transporter genes in response to ABA were also conducted (**Figure 10. *Genevestigator ABA transporter expression analyses in response to ABA.* The text on the left indicates the respective ABA treatment study. The heat map on the right indicates the ABA transporter gene expression changes in response to ABA in the respective study with down-regulated genes colored in green and up-regulated genes colored in red.**). In response to ABA, *NPF1.1*, *NPF2.5*, *NPF4.6* and *NPF5.2* were down-regulated in almost all studies. *ABCG30* was also down-regulated in a few studies. *ABCG25* and *DTX50* were strongly up-regulated and *NPF5.7* was weakly up-regulated. Gene expression of *NPF4.1*, *NPF4.2*, *NPF4.5*, *NPF4.7*, *NPF5.3* and *NPF8.2* was not affected by ABA treatment (**Figure 10. *Genevestigator ABA transporter expression analyses in response to ABA.* The text on the left indicates the respective ABA treatment study. The heat map on the right indicates the ABA transporter gene expression changes in response to ABA in the respective study with down-regulated genes colored in green and up-regulated genes colored in red.**).

Figure 10. Genevestigator ABA transporter expression analyses in response to ABA. The text on the left indicates the respective ABA treatment study. The heat map on the right indicates the ABA transporter gene expression changes in response to ABA in the respective study with down-regulated genes colored in green and up-regulated genes colored in red.
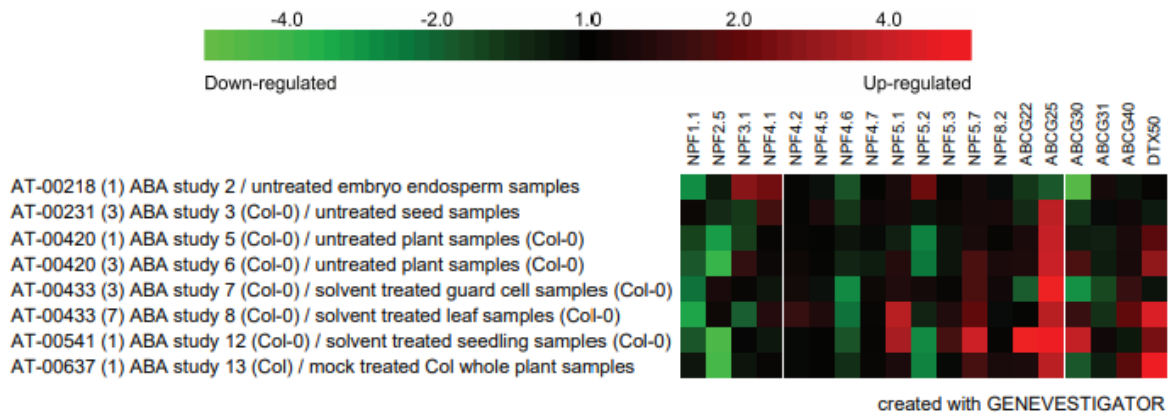
Summary

Plant hormones have an essential role in plant development, and stomatal aperture regulation. ABA is one of the most important phytohormones for stomatal regulation. To study the role of ABA transporter genes in guard cells during environmental responses, such as low humidity (high VPD), I first genotyped and isolated homozygous mutants of the ABA transporter genes *ABCG22*, *ABCG25*, *ABCG31*, *NPF4.6* and *NPF5.2*. Using these mutants and compared to Col-0 wild type Arabidopsis plants, I performed gas-exchange analyses in response to reduced air humidity and during recovery from this treatment. In my experiments I observed and could confirm previous results, showing that *ABCG22* pays a role during the low humidity response in guard cells. Compared to Col-0 wild type, the *abcg22-3* mutant closed its stomata much slower and also recovered slower from the low humidity response. Since there are a lot of ABA transporters, to develop a hypothesis about their potential function, I also checked their expression patterns using Genevestigator. I created a table of ABA transporter mutants, which indicates gene expression levels in distinct developmental stages of Arabidopsis. Among other data, I observed which transporters are highly expressed in guard cells (*NPF1.1*, *NPF4.6/AIT1*, *NPF5.1*, *NPF5.2*, *NPF5.7*, *ABCG22*, *ABCG31 and* ABCG40). From these results, we can look forward to do additional VPD response analyses and test mutants for these genes in future work.

Acknowledgements

This study was performed in The Plant Signal Research Group at the Institute of Technology.

The completion of this study could not have been possible without my supervisor Dr. Rainer Waadt. I would like to special thank him for his patience, support, and positive attitude, for his guidance and encouragement to accomplish this assignment.

I would also like to thank Prof. Dr. Hannes Kollist for providing this condition and giving me a chance to be a part of his lab group. My deepest appreciation goes to the people working in The Plant Signal Research Group, it was a great pleasure to work with them and appreciate their help, ideas, and thanks for providing such a good learning environment.

References

Ache, P., Becker, D., Ivashikina, N., Dietrich, P., Roelfsema, M.R.G., Hedrich, R., 2000. GORK, a delayed outward rectifier expressed in guard cells of Arabidopsis thaliana, is a K+-selective, K^+-sensing ion channel. FEBS Lett. 486, 93–98. https://doi.org/10.1016/S0014-5793(00)02248-1

Ali, S., Hayat, K., Iqbal, A., Xie, L., 2020. Implications of abscisic acid in the drought stress tolerance of plants. Agronomy. https://doi.org/10.3390/agronomy10091323

Araújo, W.L., Fernie, A.R., Nunes-Nesi, A., 2011. Control of stomatal aperture: A renaissance of the old guard. Plant Signal. Behav. https://doi.org/10.4161/psb.6.9.16425

Batool, S., Uslu, V.V., Rajab, H., Ahmad, N., Waadt, R., Geiger, D., Malagoli, M., Xiang, C. Bin, Hedrich, R., Rennenberg, H., Herschbach, C., Hell, R., Wirtz, M., 2018. Sulfate is incorporated into cysteine to trigger ABA production and stomatal closure. Plant Cell 30, 2973–2987. https://doi.org/10.1105/tpc.18.00612

Bauer, H., Ache, P., Lautner, S., Fromm, J., Hartung, W., Al-Rasheid, K.A.S., Sonnewald, S., Sonnewald, U., Kneitz, S., Lachmann, N., Mendel, R.R., Bittner, F., Hetherington, A.M., Hedrich, R., 2013. The stomatal response to reduced relative humidity requires guard cell-autonomous ABA synthesis. Curr. Biol. 23, 53–57. https://doi.org/10.1016/j.cub.2012.11.022

Boursiac, Y., Léran, S., Corratgé-Faillie, C., Gojon, A., Krouk, G., Lacombe, B., 2013. ABA transport and transporters. Trends Plant Sci. https://doi.org/10.1016/j.tplants.2013.01.007

Chater, C.C.C., Oliver, J., Casson, S., Gray, J.E., 2014. Putting the brakes on: Abscisic acid as a central environmental regulator of stomatal development. New Phytol. https://doi.org/10.1111/nph.12713

Chen, K., Gao, J., Sun, S., Zhang, Z., Yu, B., Li, J., Xie, C., Li, G., Wang, P., Song, C.P., Bressan, R.A., Hua, J., Zhu, J.K., Zhao, Y., 2020a. BONZAI Proteins Control Global Osmotic Stress Responses in Plants. Curr. Biol. 30, 4815-4825.e4. https://doi.org/10.1016/j.cub.2020.09.016

Chen, K., Li, G.J., Bressan, R.A., Song, C.P., Zhu, J.K., Zhao, Y., 2020b. Abscisic acid dynamics, signaling, and functions in plants. J. Integr. Plant Biol. https://doi.org/10.1111/jipb.12899

Chiba, Y., Shimizu, T., Miyakawa, S., Kanno, Y., Koshiba, T., Kamiya, Y., Seo, M., 2015.

Identification of *Arabidopsis thaliana* NRT1/PTR FAMILY (NPF) proteins capable of transporting plant hormones. J. Plant Res. 128, 679–686. https://doi.org/10.1007/s10265-015-0710-2

Choi, W.G., Miller, G., Wallace, I., Harper, J., Mittler, R., Gilroy, S., 2017. Orchestrating rapid long-distance signaling in plants with Ca^{2+}, ROS and electrical signals. Plant J. 90, 698–707. https://doi.org/10.1111/tpj.13492

Christmann, A., Weiler, E.W., Steudle, E., Grill, E., 2007. A hydraulic signal in root-to-shoot signalling of water shortage. Plant J. 52, 167–174. https://doi.org/10.1111/j.1365-313X.2007.03234.x

Cutler, S.R., Rodriguez, P.L., Finkelstein, R.R., Abrams, S.R., 2010. Abscisic acid: Emergence of a core signaling network. Annu. Rev. Plant Biol. 61, 651–679. https://doi.org/10.1146/annurev-arplant-042809-112122

Endo, A., Sawada, Y., Takahashi, H., Okamoto, M., Ikegami, K., Koiwai, H., Seo, M., Toyomasu, T., Mitsuhashi, W., Shinozaki, K., Nakazono, M., Kamiya, Y., Koshiba, T., Nambara, E., 2008. Drought induction of Arabidopsis 9-cis-epoxycarotenoid dioxygenase occurs in vascular parenchyma cells. Plant Physiol. 147, 1984–1993. https://doi.org/10.1104/pp.108.116632

Falhof, J., Pedersen, J.T., Fuglsang, A.T., Palmgren, M., 2016. Plasma Membrane H^+-ATPase Regulation in the Center of Plant Physiology. Mol. Plant. https://doi.org/10.1016/j.molp.2015.11.002

Finkelstein, R., 2013. Abscisic Acid Synthesis and Response. Arab. B. 11, e0166. https://doi.org/10.1199/tab.0166

Geiger, D., Nke Scherzer, S., Mumm, P., Stange, A., Marten, I., Bauer, H., Ache, P., Matschi, S., Liese, A., Al-Rasheid, K.A.S., Romeis, T., Hedrich, R., n.d. Activity of guard cell anion channel SLAC1 is controlled by drought-stress signaling kinase-phosphatase pair.

Zhang, H., H, Zhu, Y, P., Y, Y., S, L., L, L., 2014. A DTX/MATE-type transporter facilitates abscisic acid efflux and modulates ABA sensitivity and drought tolerance in Arabidopsis. Mol. Plant 7. https://doi.org/10.1093/MP/SSU063

Hirai, N., Yoshida, R., Todoroki, Y., Ohigashi, H., 2000. Biosynthesis of abscisic acid by the non-

mevalonate pathway in plants, and by the mevalonate pathway in fungi. Biosci. Biotechnol. Biochem. 64, 1448–1458. https://doi.org/10.1271/bbb.64.1448

Horrer, D., Flütsch, S., Pazmino, D., Matthews, J.S.A., Thalmann, M., Nigro, A., Leonhardt, N., Lawson, T., Santelia, D., 2016. Blue light induces a distinct starch degradation pathway in guard cells for stomatal opening. Curr. Biol. 26, 362–370. https://doi.org/10.1016/j.cub.2015.12.036

Hosy, E., Vavasseur, A., Mouline, K., Dreyer, I., Gaymard, F., Porée, F., Boucherez, J., Lebaudy, A., Bouchez, D., Véry, A.A., Simonneau, T., Thibaud, J.B., Sentenac, H., 2003. The Arabidopsis outward K+ channel GORK is involved in regulation of stomatal movements and plant transpiration. Proc. Natl. Acad. Sci. U. S. A. 100, 5549–5554. https://doi.org/10.1073/pnas.0733970100

Huang, S., Waadt, R., Nuhkat, M., Kollist, H., Hedrich, R., Roelfsema, M.R.G., 2019. Calcium signals in guard cells enhance the efficiency by which abscisic acid triggers stomatal closure. New Phytol. 224, 177–187. https://doi.org/10.1111/nph.15985

Imes, D., Mumm, P., Böhm, J., Al-Rasheid, K.A.S., Marten, I., Geiger, D., Hedrich, R., 2013. Open stomata 1 (OST1) kinase controls R-type anion channel QUAC1 in Arabidopsis guard cells. Plant J. 74, 372–382. https://doi.org/10.1111/tpj.12133

Inoue, S.I., Kinoshita, T., 2017. Blue light regulation of stomatal opening and the plasma membrane H^+-ATPase. Plant Physiol. 174, 531–538. https://doi.org/10.1104/pp.17.00166

Kang, J., Hwang, J.U., Lee, M., Kim, Y.Y., Assmann, S.M., Martinoia, E., Lee, Y., 2010. PDR-type ABC transporter mediates cellular uptake of the phytohormone abscisic acid. Proc. Natl. Acad. Sci. U. S. A. 107, 2355–2360. https://doi.org/10.1073/pnas.0909222107

Kang, J., Yim, S., Choi, H., Kim, A., Lee, K.P., Lopez-Molina, L., Martinoia, E., Lee, Y., 2015. Abscisic acid transporters cooperate to control seed germination. Nat. Commun. 6, 1–10. https://doi.org/10.1038/ncomms9113

Kanno, Y., Hanada, A., Chiba, Y., Ichikawa, T., Nakazawa, M., Matsui, M., Koshiba, T., Kamiya, Y., Seo, M., 2012. Identification of an abscisic acid transporter by functional screening using the receptor complex as a sensor. Proc. Natl. Acad. Sci. U. S. A. 109, 9653–9658. https://doi.org/10.1073/pnas.1203567109

Kim, T.H., Böhmer, M., Hu, H., Nishimura, N., Schroeder, J.I., 2010. Guard cell signal transduction network: Advances in understanding abscisic acid, CO_2, and Ca^{2+} signaling. Annu. Rev. Plant Biol. 61, 561–591. https://doi.org/10.1146/annurev-arplant-042809-112226

Kollist, H., Nuhkat, M., Roelfsema, M.R.G., 2014. Closing gaps: Linking elements that control stomatal movement. New Phytol. https://doi.org/10.1111/nph.12832

Kollist, T., Moldau, H., Rasulov, B., Oja, V., Rämma, H., Hüve, K., Jaspers, P., Kangasjärvi, J., Kollist, H., 2007. A novel device detects a rapid ozone-induced transient stomatal closure in intact Arabidopsis and its absence in *abi2* mutant. Physiol. Plant. 129, 796–803. https://doi.org/10.1111/j.1399-3054.2006.00851.x

Kudla, J., Becker, D., Grill, E., Hedrich, R., Hippler, M., Kummer, U., Parniske, M., Romeis, T., Schumacher, K., 2018. Advances and current challenges in calcium signaling. New Phytol. https://doi.org/10.1111/nph.14966

Kuromori, T., Miyaji, T., Yabuuchi, H., Shimizu, H., Sugimoto, E., Kamiya, A., Moriyama, Y., Shinozaki, K., 2010. ABC transporter AtABCG25 is involved in abscisic acid transport and responses. Proc. Natl. Acad. Sci. U. S. A. 107, 2361–2366. https://doi.org/10.1073/pnas.0912516107

Kuromori, T., Seo, M., Shinozaki, K., 2018. ABA Transport and Plant Water Stress Responses. Trends Plant Sci. https://doi.org/10.1016/j.tplants.2018.04.001

Kuromori, T., Sugimoto, E., Shinozaki, K., 2011. Arabidopsis mutants of AtABCG22, an ABC transporter gene, increase water transpiration and drought susceptibility. Plant J. 67, 885–894. https://doi.org/10.1111/j.1365-313X.2011.04641.x

Lee, K.H., Piao, H.L., Kim, H.Y., Choi, S.M., Jiang, F., Hartung, W., Hwang, Ildoo, Kwak, J.M., Lee, I.J., Hwang, Inhwan, 2006. Activation of Glucosidase via Stress-Induced Polymerization Rapidly Increases Active Pools of Abscisic Acid. Cell 126, 1109–1120. https://doi.org/10.1016/j.cell.2006.07.034

Leung, J., Giraudat, J., 1998. Abscisic acid signal transduction. Annu. Rev. Plant Biol. 49, 199–222. https://doi.org/10.1146/annurev.arplant.49.1.199

Lin, Z., Li, Y., Zhang, Z., Liu, X., Hsu, C.C., Du, Y., Sang, T., Zhu, C., Wang, Y., Satheesh, V., Pratibha, P., Zhao, Y., Song, C.P., Tao, W.A., Zhu, J.K., Wang, P., 2020. A RAF-SnRK2

kinase cascade mediates early osmotic stress signaling in higher plants. Nat. Commun. 11. https://doi.org/10.1038/s41467-020-14477-9

Ma, Y., Szostkiewicz, I., Korte, A., Moes, D., Yang, Y., Christmann, A., Grill, E., 2009. Regulators of PP2C phosphatase activity function as abscisic acid sensors. Science. 324, 1064–1068. https://doi.org/10.1126/science.1172408

Merilo, E., Jalakas, P., Kollist, H., Brosché, M., 2015a. The Role of ABA recycling and transporter proteins in rapid stomatal responses to reduced air humidity, elevated CO_2, and exogenous ABA. Mol. Plant. https://doi.org/10.1016/j.molp.2015.01.014

Merilo, E., Jalakas, P., Laanemets, K., Mohammadi, O., Hõrak, H., Kollist, H., Brosché, M., 2015b. Abscisic acid transport and homeostasis in the context of stomatal regulation. Mol. Plant. https://doi.org/10.1016/j.molp.2015.06.006

Meyer, S., Mumm, P., Imes, D., Endler, A., Weder, B., Al-Rasheid, K.A.S., Geiger, D., Marten, I., Martinoia, E., Hedrich, R., 2010. AtALMT12 represents an R-type anion channel required for stomatal movement in Arabidopsis guard cells. Plant J. 63, 1054–1062. https://doi.org/10.1111/j.1365-313X.2010.04302.x

Nakashima, K., Yamaguchi-Shinozaki, K., Shinozaki, K., 2014. The transcriptional regulatory network in the drought response and its crosstalk in abiotic stress responses including drought, cold, and heat. Front. Plant Sci. https://doi.org/10.3389/fpls.2014.00170

Negi, J., Matsuda, O., Nagasawa, T., Oba, Y., Takahashi, H., Kawai-Yamada, M., Uchimiya, H., Hashimoto, M., Iba, K., 2008. CO_2 regulator SLAC1 and its homologues are essential for anion homeostasis in plant cells. Nature 452, 483–486. https://doi.org/10.1038/nature06720

Pilot, G., Lacombe, B., Gaymard, F., Chérel, I., Boucherez, J., Thibaud, J.B., Sentenac, H., 2001. Guard Cell Inward K^+ Channel Activity in Arabidopsis Involves Expression of the Twin Channel Subunits KAT1 and KAT2. J. Biol. Chem. 276, 3215–3221. https://doi.org/10.1074/jbc.M007303200

Roelfsema, M.R.G., Hanstein, S., Felle, H.H., Hedrich, R., 2002. CO_2 provides an intermediate link in the red light response of guard cells. Plant J. 32, 65–75. https://doi.org/10.1046/j.1365-313X.2002.01403.x

Sasaki, T., Mori, I.C., Furuichi, T., Munemasa, S., Toyooka, K., Matsuoka, K., Murata, Y.,

Yamamoto, Y., 2010. Closing plant stomata requires a homolog of an aluminum-activated malate transporter. Plant Cell Physiol. 51, 354–365. https://doi.org/10.1093/pcp/pcq016

Sato, A., Sato, Y., Fukao, Y., Fujiwara, M., Umezawa, T., Shinozaki, K., Hibi, T., Taniguchi, M., Miyake, H., Goto, D.B., Uozumi, N., 2009. Threonine at position 306 of the KAT1 potassium channel is essential for channel activity and is a target site for ABA-activated SnRK2/OST1/SnRK2.6 protein kinase. Biochem. J. 424, 439–448. https://doi.org/10.1042/BJ20091221

Schroeder, J.I., Allen, G.J., Hugouvieux, V., Kwak, J.M., Waner, D., 2001. Guard cell signal transduction. Annu. Rev. Plant Biol. 52, 627–658. https://doi.org/10.1146/annurev.arplant.52.1.627

Schwartz, S.H., Qin, X., Zeevaart, J.A.D., 2003. Update on Abscisic Acid Biosynthesis Elucidation of the Indirect Pathway of Abscisic Acid Biosynthesis by Mutants, Genes, and Enzymes 1. https://doi.org/10.1104/pp.102.017921

Shinozaki, K., Yamaguchi-Shinozaki, K., 2000. Molecular responses to dehydration and low temperature: differences and cross-talk between two stress signaling pathways. Curr. Opin. Plant Biol. 3, 217–223. https://doi.org/10.1016/s1369-5266(00)80068-0

Siegel, R.S., Xue, S., Murata, Y., Yang, Y., Nishimura, N., Wang, A., Schroeder, J.I., 2009. Calcium elevation-dependent and attenuated resting calcium-dependent abscisic acid induction of stomatal closure and abscisic acid-induced enhancement of calcium sensitivities of S-type anion and inward-rectifying K^+ channels in Arabidopsis guard cells. Plant J. 59, 207–220. https://doi.org/10.1111/j.1365-313X.2009.03872.x

Sierla, M., Hõrak, H., Overmyer, K., Waszczak, C., Yarmolinsky, D., Maierhofer, T., Vainonen, J.P., Salojärvi, J., Denessiouk, K., Laanemets, K., Tõldsepp, K., Vahisalu, T., Gauthier, A., Puukko, T., Paulin, L., Auvinen, P., Geiger, D., Hedrich, R., Kollist, H., Kangasjärvi, J., 2018. The receptor-like pseudokinase GHR1 is required for stomatal closure. Plant Cell 30, 2813–2837. https://doi.org/10.1105/tpc.18.00441

Sirichandra, C., Gu, D., Hu, H.C., Davanture, M., Lee, S., Djaoui, M., Valot, B., Zivy, M., Leung, J., Merlot, S., Kwak, J.M., 2009. Phosphorylation of the Arabidopsis AtrbohF NADPH oxidase by OST1 protein kinase. FEBS Lett. 583, 2982–2986. https://doi.org/10.1016/j.febslet.2009.08.033

Soma, F., Takahashi, F., Suzuki, T., Shinozaki, K., Yamaguchi-Shinozaki, K., 2020. Plant Raf-like kinases regulate the mRNA population upstream of ABA-unresponsive SnRK2 kinases under drought stress. Nat. Commun. 11. https://doi.org/10.1038/s41467-020-15239-3

Sussmilch, F.C., McAdam, S.A.M., 2017a. Surviving a dry future: Abscisic acid (ABA)-mediated plant mechanisms for conserving water under low humidity. Plants. https://doi.org/10.3390/plants6040054

Takahashi, F., Kuromori, T., Sato, H., Shinozaki, K., 2018a. Regulatory gene networks in drought stress responses and resistance in plants, in: Advances in Experimental Medicine and Biology. Springer New York LLC, pp. 189–214. https://doi.org/10.1007/978-981-13-1244-1_11

Takahashi, F., Kuromori, T., Sato, H., Shinozaki, K., 2018b. Regulatory gene networks in drought stress responses and resistance in plants, in: Advances in Experimental Medicine and Biology. Springer New York LLC, pp. 189–214. https://doi.org/10.1007/978-981-13-1244-1_11

Takahashi, F., Suzuki, T., Osakabe, Y., Betsuyaku, S., Kondo, Y., Dohmae, N., Fukuda, H., Yamaguchi-Shinozaki, K., Shinozaki, K., 2018c. A small peptide modulates stomatal control via abscisic acid in long-distance signaling. Nature 556, 235–238. https://doi.org/10.1038/s41586-018-0009-2

Takahashi, Y., Ebisu, Y., Kinoshita, T., Doi, M., Okuma, E., Murata, Y., Shimazaki, K.I., 2013. BHLH transcription factors that facilitate K^+ uptake during stomatal opening are repressed by abscisic acid through phosphorylation. Sci. Signal. 6. https://doi.org/10.1126/scisignal.2003760

Takahashi, Y., Zhang, J., Hsu, P.K., Ceciliato, P.H.O., Zhang, L., Dubeaux, G., Munemasa, S., Ge, C., Zhao, Y., Hauser, F., Schroeder, J.I., 2020. MAP3Kinase-dependent SnRK2-kinase activation is required for abscisic acid signal transduction and rapid osmotic stress response. Nat. Commun. 11. https://doi.org/10.1038/s41467-019-13875-y

Vahisalu, T., Kollist, H., Wang, Y.F., Nishimura, N., Chan, W.Y., Valerio, G., Lamminmäki, A., Brosché, M., Moldau, H., Desikan, R., Schroeder, J.I., Kangasjärvi, J., 2008. SLAC1 is required for plant guard cell S-type anion channel function in stomatal signalling. Nature 452, 487–491. https://doi.org/10.1038/nature06608

Xu, Z.Y., Lee, K.H., Dong, T., Jeong, J.C., Jin, J.B., Kanno, Y., Kim, D.H., Kim, S.Y., Seo, M., Bressan, R.A., Yun, D.J., Hwang, I., 2012. A vacuolar β-Glucosidase homolog that possesses glucose-conjugated abscisic acid hydrolyzing activity plays an important role in osmotic stress responses in Arabidopsis. Plant Cell 24, 2184–2199. https://doi.org/10.1105/tpc.112.095935

Yamauchi, S., Takemiya, A., Sakamoto, T., Kurata, T., Tsutsumi, T., Kinoshita, T., Shimazaki, K.I., 2016. The plasma membrane H$^+$-ATPase AHA1 plays a major role in stomatal opening in response to blue light. Plant Physiol. 171, 2731–2743. https://doi.org/10.1104/pp.16.01581

NON-EXCLUSIVE LICENCE TO REPRODUCE THESIS AND MAKE THESIS PUBLIC

I, **Turgay Hasanov**,

1. herewith grant the University of Tartu a free permit (non-exclusive licence) to

reproduce, for the purpose of preservation, including for adding to the DSpace digital archives until the expiry of the term of copyright,

The function of ABA transporters during low humidity-induced stomatal closure in *Arabidopsis thaliana*,

supervised by Dr. Rainer Waadt, Prof. Dr. Hannes Kollist.

2. I grant the University of Tartu a permit to make the work specified in p. 1 available to the public via the web environment of the University of Tartu, including via the DSpace digital archives, under the Creative Commons licence CC BY NC ND 3.0, which allows, by giving appropriate credit to the author, to reproduce, distribute the work and communicate it to the public, and prohibits the creation of derivative works and any commercial use of the work until the expiry of the term of copyright.

3. I am aware of the fact that the author retains the rights specified in p. 1 and 2.

4. I certify that granting the non-exclusive licence does not infringe other persons' intellectual property rights or rights arising from the personal data protection legislation.

Turgay Hasanov

20/05/2021